Inorganic Nanoparticles Based Contrast Agents for X-ray Computed Tomography

ARTICLE · JULY 2012

DOI: 10.1002/adhm.201200032 · Source: PubMed

3 AUTHORS:

Anshuman Jakhmola
University of Kentucky
11 PUBLICATIONS **161** CITATIONS
SEE PROFILE

Nicolas Anton
University of Strasbourg
59 PUBLICATIONS **1,358** CITATIONS
SEE PROFILE

Thierry Vandamme
University of Strasbourg
91 PUBLICATIONS **1,526** CITATIONS
SEE PROFILE

Inorganic Nanoparticles Based Contrast Agents for X-ray Computed Tomography

Anshuman Jakhmola, Nicolas Anton, and Thierry F. Vandamme*

Nanomaterials have gained considerable attention and interest in the development of new and efficient molecular probes for medical diagnosis and imaging. Heavy metal nanoparticles as such are excellent absorber of X-rays and can offer excellent improvement in medical diagnosis and X-ray imaging. Substantial progress has been made in the synthesis protocol and characterization studies of these materials but a major challenge still lies in the toxicological studies, which are rather incomplete. The worst known cases were those associated with Thorotrast (suspension of ThO_2 nanoparticles) which resulted in many deaths over years. Properly protected nanomaterials conjugated or coated with biocompatible materials can be used for the fabrication of various functional systems with multimodality, targeting properties, reduced toxicity and proper removal from the body. This review aims mainly to provide the advances in the development of inorganic nanoparticle based X-ray contrasting agents with an overview of methods of their preparation, functionalization and applications in medical diagnosis.

1. Introduction

The efficient use of X-rays for imaging and computed tomography applications not only depends on the advancement of diagnostic equipment but also on the contrasting media necessary to generate two and three dimensional images for *in vivo* biomedical applications. Historically, the importance of X-rays in medical diagnosis and imaging was soon recognized after their discovery in 1895 by Rontgen, and research on contrast media and medical imaging was started soon thereafter. The use of the first positive contrast agent most probably dates back to 1896 when barium sulfate was used for investigation of peristalsis movement in animals;[1] later in 1921 iodized oil Lipodol (iodized poppy seed oil) was introduced as first suitable X-ray contrast media in myelography.[2] Although X-ray computed tomography is considered as one of the most important imaging techniques for various medical, scientific and technological applications, its use is quite limited as compared to other imaging techniques like MRI or fluorescence imaging. Major limitations are often associated with contrasting agents approved for medical diagnosis. Modern X-ray contrasting agents approved for clinical use are either barium sulfate based solution or poly-iodinated aromatic compounds. Conventional ionic contrast media, which are sodium and meglumine salts of tri-iodinated benzoic acid were introduced more than 50 years ago and were quite hyperosmolar and greatly increased toxic and side effects in patients. With new developments, major improvements were achieved in terms of the chemistry and physiological compatibility of these solutions to reduce the side effects. However, still to date their processing and synthesis require complex methodologies that are performed under stringent and toxic conditions. Besides, these tri-iodobenzene based agents are small molecular weight hydrophilic molecules, which exhibit a rapid renal clearance and vascular permeation. While traditional clinical CT scanners are quite effective for routine diagnosis due to their small response time (*e.g.* five seconds to acquire 15 cm thick volume), MicroCT systems tend to be quite slow in comparison (*e.g.* ten minutes to scan a mouse); As a result, these are unsuitable for most non preclinical X-ray imaging experiments and analysis. With time many formulation and chemical strategies were undertaken in order to increase the half-life of iodinated contrasting agents. For instance one such development was the introduction of nanoparticle based iodinated molecules as blood pool contrasting agents (BPCA). BPCA are systems which remain in the blood for a prolonged period of time as compared with conventional contrast agents, which diffuse quickly into the interstitial space. These systems, in the form of nanoparticles with a controlled functionalization and surface coating provide significant stealth and antibiofouling properties towards the immune system. In fact this mixed nature of the structure not only increases their residence time in blood but subsequently enhances the contrast. We have recently reviewed iodinated blood pool contrast agents in detail,[3] covering all their chemical and physicochemical properties: surface functionalization, stability, toxicology and pharmacokinetics. These contrasting agents which are mainly in the form of colloidal solutions may contain liposomes (encapsulating small molecular weight iodinated molecules), nano-emulsions, micelles, dendrimers and

A. Jakhmola, N. Anton, T. F. Vandamme
University of Strasbourg
Faculté de Pharmacie
74 route du Rhin, BP 60024
F-67401 Illkirch Cedex, France
CNRS 7199, Laboratoire de Conception et Application de Molécules Bioactives
équipe de Pharmacie Biogalénique
E-mail: nanton@unistra.fr

DOI: 10.1002/adhm.201200032

polymeric nanoparticles.[3] The limited stability and need to be administrated in significant amounts (in comparison to other imaging techniques, e.g., MRI) due to the limitation of iodine loading in the particles are the major drawbacks faced by these systems.

While processes have been evolutionarily developed for production of new and better iodinated contrasting agents with exquisite control over osmolality, toxicity etc. there are still no real developments that overcome limitations associated with low attenuation coefficient and non-targeting nature as contrast agents cannot be conjugated to most biological components. Other limitations includes (i) toxicity- in certain cases, renal toxicity, kidney failure, anaphylactic shocks have been reported,[4] (ii) high osmolality and viscosity can also cause certain adverse side effects, (iii) medium molecular weight of iodinated and barium compounds which limits their use with high energy X-rays. The general overview of the computed assisted X-ray tomography is presented in **Figure 1**.

In contrast, alternative emerging solutions are being developed, and applied in the field of X-ray imaging. The propose is to use standard synthetic procedure, either from bottom up or top down, inorganic surface-functionalized nanoparticles as long circulation and/or targeted CT contrast agents. As such they appear quite promising, and researches on them are extremely dynamic in nature, particularly with gold nanoparticles which possess high contrasting abilities and constitute nearly half of the total publications on X-ray imaging. Other different types of inorganic nanoparticles include heavy metals like silver, platinum, bismuth, gadolinium etc. which also have been reviewed in detail.[5] Beyond simple materials fabrication, the advantages of inorganic nanoparticles in comparison to iodinated compounds are numerous, including substantial control in the synthetic process and higher X-ray absorption coefficient giving rise to greater contrast, and thus a reduction in the dosage amount. The nucleation, growth and control of the bioconjugation chemistry of these inorganic materials are simpler and are easily adaptable to specific targeting agent. These materials provide unique and fascinating architectures as programmable probes and preliminary *in vitro* and *in vivo* experiments on lab animals have shown very interesting and controlled possibilities.

In this review we will focus on the recent research efforts based on inorganic nanoparticles as contrasting agents for X-ray computed tomography and X-ray imaging. We will survey different types of nanomaterials based on metals, alloys, oxides, sulfides, of interest. We expect this to be interesting and informative for researchers working in the field of nanotechnology and contrasting agents.

1.1. Physical Principles

The function of a contrast agent is to increase the visibility of internal body structure by changing the contrast between different tissues. Contrast between tissues arises from different attenuation of X-rays as they pass through the body to the detector. To fulfill this requirementk, any X-ray contrast medium must differ in X-ray attenuation from the surrounding tissue or organ. Basically contrasting agents absorb X-rays either more or less than body constituents particularly water. The absorption of X-rays by any material preliminary depends upon the mass absorption coefficient of the elements present in the contrast media as well as other factors like concentration, thickness of sample and energy of X-rays etc.

Anshuman Jakhmola obtained his PhD in Chemistry in 2008 from the Indian Institute of Technology Roorkee. Then, he worked as Research associate in the Department of Chemistry, University of Kentucky (2009) and in the Faculty of Pharmacy, University of Strasbourg (2010-). His experience mainly focused on research projects from conception to implementation, on nanotechnology, inorganic chemistry and physical/surface chemistry applied to biomedical sciences.

Nicolas Anton is currently Assistant Professor at the University of Strasbourg, France. He prepared his PhD in Physcical Chemistry in 2007 from the University of Angers (team of Pr. J.-P. Benoit), and was research fellows 2008 with Pr. J. Bibette at ESPCI, Paris. In 2008, he joined the team of Pr. T. Vandamme in Strasbourg as Assistant Professor. From an initial formation in general Physics and Chemistry, and he developed an expertise in Physical Chemistry of colloids and interfaces applied to biomedical sciences, innovative drug delivery systems and contrast agents.

Thierry Vandamme obtained his PhD in Pharmaceutical Sciences in 1994 at the catholic University of Louvain in Belgium. After two post-doctoral training courses (in the Laboratory of Dr. Jorge Heller and in the research team of Professor Ruth Duncan), he joined the University of Strasbourg as lecturer where he was promoted Professor in Biogalenics in 2005. The main aim of his research activities are based on the developments of new drug delivery systems.

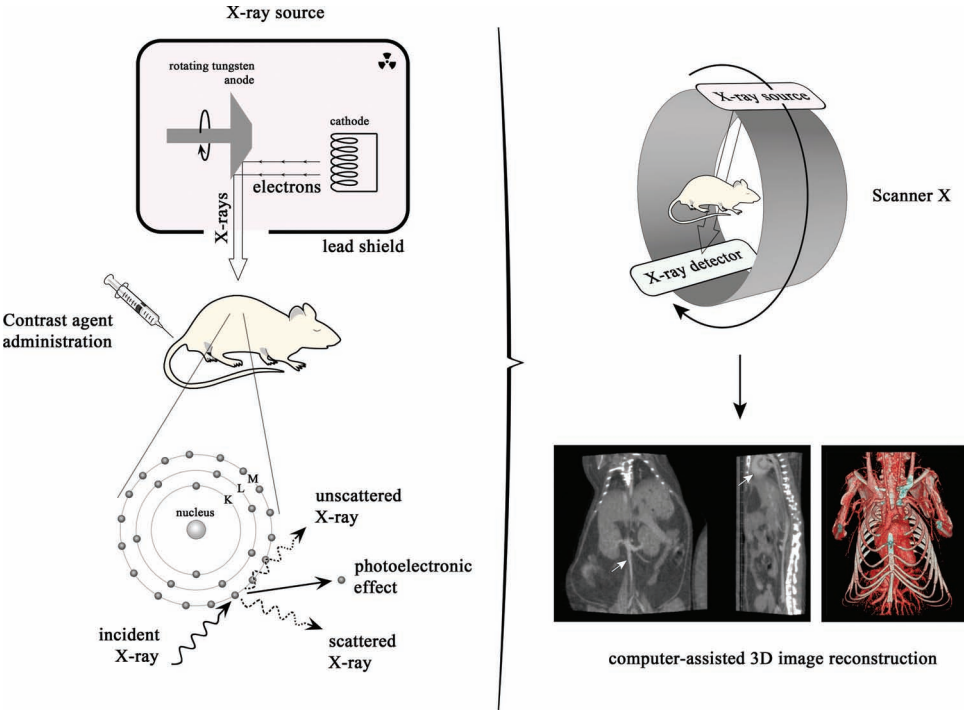

Figure 1. Schematic diagram and basic principles of computed assisted tomography.

When a parallel beam of X-rays passes through a layer of matter of thickness X, a part of it passes directly through it without any interaction (primary radiation), while a certain fraction of it is absorbed, deflected or scattered. The intensity of transmitted beam J through this layer is related with the intensity of incident beam (J_0) in according to Beer–Lambert law given by equation,

$$J = J_0 \exp^{\frac{\mu \cdot m}{\rho}}$$

where μ/ρ is known as the mass attenuation coefficient which is directly dependent on the energy of incident X-rays and the mass m of different elements present in the material. Keeping other factors constant, the mass attenuation coefficient tends to increase with increase in atomic number of elements in periodic table, and decrease with increase in energy of X-rays. Many theoretical and experimental based studies have also shown that elements with higher atomic number than iodine demonstrate superior X-ray attenuation ability at normal or even higher operating tube voltages due to the higher K-edges of heavy elements. The K-edges of heavy elements lies within the diagnostic X-ray spectrum as such an abrupt increase in attenuation at discrete energies near the K-edge is observed (see below). Thus a contrast media based on elements with higher atomic number will be more advantageous in terms of intrinsic contrast, lower dose requirement and lower radiation exposure to patients.

1.2. Basic Requirements for X-ray Contrast Media

In order to get sufficient contrast in comparison to the background, a high concentration of contrast media is required, as such the most basic requirement for contrast media is its biocompability and inertness with living tissue. Although the currently available iodinated compounds have fulfilled these basic requirements, their use is largely based on low toxicity and cost effectiveness rather than high radiopacity for X-rays. The main requirements of an X-ray contrast agent are as follows:

- High Solubility: For intravenous administration, any X-ray contrasting agent must have high solubility as very high concentration is needed to compensate for the most relevant drawback of X-rays, which is the low contrast sensitivity.
- Chemical stability: They must be chemically stable and pharmacologically inert after intravenous administration and must not react, coagulate or metabolize once administrated intravenously.
- Opacity: The contrast media must have high efficiency as X-ray attenuators. Higher X-ray attenuation means higher contrast enhancement at lower dosage levels.
- Toxicity/tolerability: The osmolality, viscosity and pH must be comparable to that of body fluids and toxicity (chemotoxicity and osmotoxicity) must be as low as possible.

2. Noble Metal Based Nanoparticles

Noble metal nanoparticles are versatile agents with a variety scientific and technological applications. The intense interest derives from their unique characteristics: controlled morphologies, spatial charge confinement, ease of synthesis, and facile

surface chemistry and functionalization. Gold and silver nanoparticles have been used for centuries in many countries to cure certain diseases,[6] however their use in the field of X-ray imaging is quite new and one of the most notable applications. Beyond simple fabrication process, recent research efforts points towards their exciting opportunities in the field of CT imaging. In fact gold nanoparticles have shown quite positive results to overcome current limitations and are expected to enter clinical applications and diagnoses in near future.

2.1. Gold Nanoparticles as CT Contrast Agents

Nanogold which is known since ancient times for their metaphysical and healing powers is one of the most extensively studied nanomaterial which has a long history of synthesis and biomedical applications. In 2004 Hainfeld and his team, exploited the high atomic weight of gold in the field of X-ray imaging which has gained considerable momentum worldwide.[7] It can be clearly seen that since 2004, most of the research investigations on inorganic nanoparticles based X-ray contrasting media are focused on gold nanoparticles or their hybrids. Beside the fact that gold particles displays a strong attenuation in X-ray region, research have also been focused on the substantial control of their physical, chemical and biological properties which makes it one of the most ideal candidate for X-ray CT and multimodal imaging.[8] AuNPs are not only stable and inert, but they also present much more fascinating properties such as their self-assembly in conjugation with organization motifs and templates, size-related electronic and optical properties (quantum-size effect), and their applications in catalysis and biological process. The applications of AuNPs for medical diagnosis and X-ray CT imaging, can be briefly summarized into following points: (i) X-ray attenuation or radiopacity properties, which have emerged as better and higher than conventional CT contrast agent (*e.g.* iodinated), (ii) a highly flexible facile surface chemistry which allows a wide modularity in the surface functionalization for *in vivo* stabilization or coating (with antibiofouling agents, *e.g.* polyethylene glycol), and conjugating with specific functional molecules for active targeting to specified organs, regions, or cancerous cells (tumor) (*e.g.* antibody, peptides, etc. see below), (iii) and *in vivo* nontoxic and biocompatible properties.

2.1.1. Synthesis of Gold Nanoparticles

While the first formulation of gold nanoparticles dates back around 5*th* century BC, in literature it was not until 1847 when Faraday first reported the formation of deep red solutions of colloidal gold by aqueous reduction of gold chloride ($AuCl^{4-}$) by phosphorus in CS_2 (carbon disulfide). The modern synthesis protocol are also based on a reduction of gold salt by a variety of reduction agents and involves well-described chemical methods, which can also potentially include their functionalization, coating or conjugation with active molecules. This section will first focus on a global presentation of the chemical strategies commonly undertaken for the formulation of gold colloids for X-ray imaging, followed by a brief description of their applications in X-ray imaging and finally a discussion of the impact of the formulation parameters, chemistry, and coating/targeting agents on their X-ray attenuation properties, stability and other physical properties. Next, we will discuss the extent in which these AuNPs can offer a plethora of new diagnosis and/or therapeutics tools, where the field of applications (*e.g.* the *in vivo* targeting) will be directly related to the chemical nature of the coating agents. In this part, we will specifically focus on the supramolecular chemistry aiming at surface functionalization, by reviewing the results obtained with the combination of CT imaging and active targeting of tumors and specific organs.

Citrate reduction: This method pioneered by J. Turkevich in 1951[6,9] is still one of the most adopted method for the formulations of AuNPs for CT imaging.[10–16] The synthesis protocol is one of the simplest where citrate is used both as a reducing and stabilizing agent to produce more or less monodisperse spherical gold nanoparticles with a size range of about 10–20 nm. Further control of particle size and range can easily be carried out by a using a much improved method,[17,18] with size tunable from 16 to 147 nm. Recent works[19] have shown that, size can also be controlled by the addition of an amphiphile into the nanoparticle synthesis reaction, and can be accurately controlled by manipulating amphiphile-to-gold ratio. The major advantage of this method is that the surface functionalization is not very strong and can be easily replaced by other ligands. As such the citrate molecules can be easily replaced with a variety of materials depending upon aimed applications, for instance, in CT imaging, replacement with a variety of biocompatible materials or functional molecules have shown quite impressive results.[10–16]

Two-phase synthesis: The Burst-Schiffrin method. This method is based on reduction of gold ions in an organic phase in presence of specific thiolated compounds like lipids, lipophilic surfactants, alkanethiols, for *e.g.* dodecanethiol. The binding of thiols with gold nanoparticles is particularly strong due to the soft nature of both Au and S. The process, inspired by the Faraday's two-phase system,[20] involves the use of tretraoctylammonium bromide to transfer $AuCl^-$ ions into the organic phase (*e.g.* toluene), which is then reduced instantaneously by $NaBH_4$. The AuNPs typically show a size in the range 1–5.2 nm but the size and/or size distribution can easily be modified by manipulating experimental conditions like thiol/gold mole ratios, rate of addition of reducing agent, temperature and the nature of the thiol ligands.[21–27] The great advantage offered by this technology definitely lies in the stability of the AuNPs. This synthesis process results in the formulation of thermally and air-stable gold nanoparticles, which can be repeatedly isolated and redissolved in common organic solvents without irreversible aggregation or decomposition. This also enables easy particles handling and besides, this method is quite interesting as it allows a simple route to functionalize AuNPs, performed by an "exchange" of the adsorbed alkanethiol for functionalized aklanethiol.[27–30] Other different sulfur-containing compounds[31–40] and ligands like phosphine, phosphine oxide, amine and carboxilates were also used in this biphasic formulation method.[41–49] These systems allowed the fabrication of AuNPs with sizes significantly higher than above, *e.g.* 12, 28, 42 nm for PPh_3 or 8.59 nm[42] using octadecylamine.[47]

In situ synthesis in colloidal template: Microemulsions are thermodynamically stable systems which are able to develop a large

oil/water interface through the formation of nano-scale system, *e.g.* swollen micelles.[50] In the fabrication of AuNPs, these dispersed systems have been used as "nano-reservoirs" in the presence or absence of thiol ligands, in which the transfer of the gold ions from the aqueous to the organic phase is enhanced by the large interfacial area.[51–58]

Other methods: The seeding growth method for generating AuNPs by step-by-step process is also a popular technique which offers the possibility to control the size distribution (5 to 40 nm),[59–61] and has been widely used for the fabrication of gold nanorods.[62] Besides the thermodynamical parameters influencing the AuNPs synthesis, numerous physical phenomenon like UV, near-IR irradiations, ultrasounds, γ-irradiation, etc. also displays a significant impact on the physicochemical properties of the nanoparticles (reviewed in detail, along with additional AuNPs fabrication and stabilization techniques, in Ref. 6).

In situ synthesis in dendrimers: The use of dendrimers as templates for entrapping[63–65] or stabilizing[66–70] AuNPs is very popular for biomedical applications, and occupies a significant role in the fabrication of gold nanoparticle based contrasting agents for X-ray *in vivo* imaging applications.[63,64,71–74] The synthesis protocol is quite similar to the methods described above, as the dendrimer's cores present sites with affinities for the gold ions Au^{3+}. The fabrication of dendrimer-entrapped gold nanoparticles (AuDENPs) is generally performed by the reduction of $HAuCl_4$ by $NaBH_4$ in a mixture of water/methanol.[63,64,71,72] The evident advantage of this method is a simple synthesis route with full control of the surface chemistry, *i.e* the control of the toxicity, of the long circulation properties and targeting properties. In this respect, the dendrimer chemistry allow to synthesize AuDENPs with terminal amines transformed to acetyl functional groups, significantly avoiding nonspecific cell membrane binding and toxicity.[68,73,75–77] Likewise, the amine-terminated gold-loaded dendrimers can serve as a platform for conjugation with targeting ligands;[73,77] however pre-modified dendrimers with targeting moieties can be also used for the AuDENPs preparation.[68]

Typical examples of gold nano-colloids obtained with the methods described above are illustrated in **Figure 2** below.

2.1.2. Why are AuNPs Best Suited for X-ray Imaging?

Globally, most work reported in the last decade focuses on the applications of gold nanoparticles for X-ray imaging. There are several basic advantages of these systems in comparision to the traditional iodine-based contrast agents like exceptional stability against oxidation, higher Z-number and absorption coefficient,[4] that is to say, respectively, gold: 79 and 5.16 cm^2g^{-1}, iodine: 53 and 1.94 cm^2g^{-1} (absorption coefficient at 100 keV; for comparison, water absorption is 0.171 cm^2g^{-1}). As a result, gold provides 2.7 times more contrast per unit weight than iodine. Moreover, gold imaging around 80–100 keV also reduces interferences from bone and soft tissues absorption and this subsequently reduces the overall radiation dosage and exposure. **Figure 3** reports the comparison of mass attenuation coefficients plotted against the photon energy for different materials used for in the fabrication of BPCA (iodine, gold and bismuth) compared to blood, soft tissues, bones, and water.

It can be clearly seen that the greater contrast of inorganic compounds in the measuring zone comes from the sharp increase of the mass attenuation coefficients, (photoelectron effect) at metal K-edge energies, *i.e.* the electronic transitions can only exist above these thresholds energies, resulting in sharp "jumps" in their X-ray attenuation profiles. In this way, it can be clearly seen that in order to maximize the efficiency, gold must be used at energies higher than ~80 keV. Accordingly, numerous publications have compared the *in vivo* contrast of inorganic nanoparticles with traditional iodinated compounds, highlighting some "equivalent concentrations" which provides the same X-ray attenuation (depending on the experimental conditions like photon energy as shown in Figure 3), for example the contrast of heparin-coated AuNPs (at 15.7 mg $Au \cdot mL^{-1}$) was found to be equivalent to eXIA 160 (at 53.3 mg $I \cdot mL^{-1}$).[88] Similarly 1.27 M of PEG-coated AuNPs gave Hounsfield unit (HU) value (around 6690 HU) which is equivalent to 2.36 M (≡ 300 mg $I \cdot mL^{-1}$) of Ultravist(a conventional iodinated contrast agent).[10] There are various other examples in literature[11,64,88] but such results are not only dependent on concentration chosen for the *in vivo* dose but are also affected by particle size, experimental parameter, and acquisition protocol. At a given energy, the photon absorption is linearly dependent to the concentration, thus exhibiting different slopes in function of the metal (as illustrated in Ref. 64 for instance). At this point, a great challenge is to define a compromise between the best contrast agent loading or concentration, or the higher tolerance and the lower toxicity.

2.1.3. In vitro and in vivo Imaging and/or Targeted-Imaging with AuNPs

Most of the work published on gold nanoparticles for X-ray imaging applications is aimed on the fabrication, coating, targeting and biological evaluation, however only a few actually emphasize on *in vivo* imaging. After the pioneer work by Hainfeld *et al.* in 2006[4] in which they proposed a 2-dimensions projection of mice carried out with a mammography unit (with 8 mAs exposures, 0.4 s at 22 kVp), it was almost after one year when Kim *et al.*[10] and Cai *et al.*[11] reported the in vivo applications of AuNPs as X-ray contrast agents with micro computed tomography. Both these authors used PEGylted AuNPs as BPCA, which provided significant vascular contrast enhancement with plasma half-time around 12 h in[10] and at 14.6 h in[11]. After that, most published works presenting *in vivo* applications of AuNPs as X-ray contrast agents are quite new, published mostly in 2010 and 2011. It can be seen that after intravenous injection these nanoparticulate systems can exhibit a wide range applications depending on coating agents for example vascular imaging as BPCA,[13,63,64,89] liver or spleen imaging,[12,71,88,90] or even tumor-specific targeting imaging after i.p.[91] or i.v.[14] administration (generally with BPCA properties form enhancing the targeting properties). As emphasized above, the great advantages of gold nanoparticles (AuNPs), lies in their highly flexible surface supramolecular chemistry, enabling the fabrication of hybrid or conjugated nanoparticles, by coating or binding them with specific biomolecules or targeting agents, which may include, monoclonal antibodies, aptamers, peptides, and various receptor-specific surfaces.[92–97] Actually, the coating of AuNPs

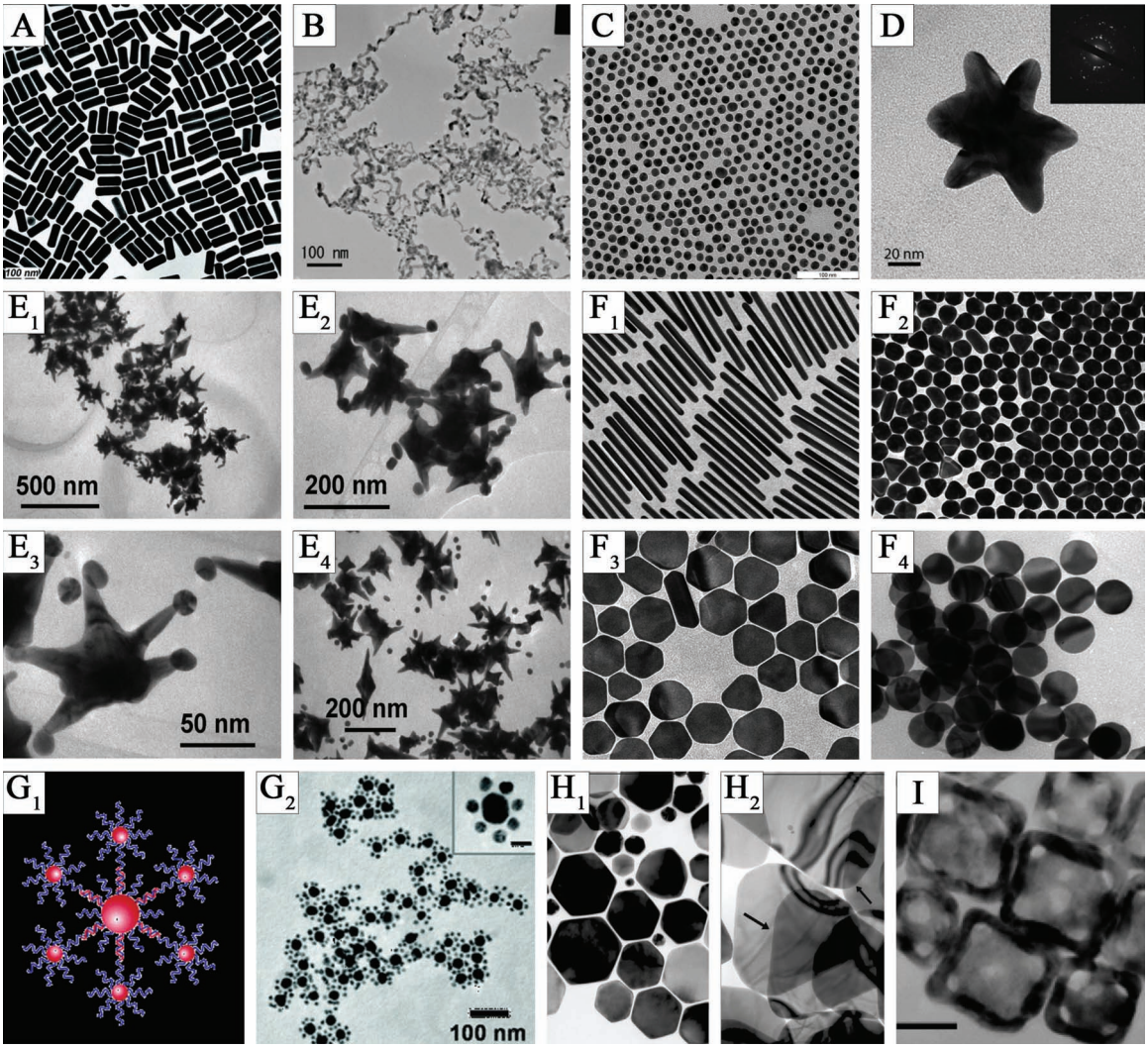

Figure 2. Nano gold – Different morphologies ((A) Nanorods. Reproduced with permission.[78] Copyright 2008, American Chemical Society. (B) Gold Nanowires, Reproduced with permission.[79] Copyright 2004, American Chemical Society. (C) Monodisperse Gold Nanoparticles. Reproduced with permission.[80] Copyright 2010, American Chemical Society. (D) Star-Shaped Gold Nanoparticles. Reproduced with permission.[81] Copyright 2006, American Chemical Society. (E) Nanobranches and Nanospheres. Reproduced with permission.[82] Copyright 2009, American Chemical Society. (F) Nanorods, Nanospheres and Faceted platelets. Reproduced with permission.[83] Copyright 2008, American Chemical Society (ACS). (G) Satellite type structure. Reproduced with permission.[84] Copyright 2006. American Chemical Society (ACS). (H) Large polygons. Reproduced with permission.[85] Copyright 2007, American Chemical Society (ACS), (I) Nanocages. Reproduced with permission.[86] Copyright 2007, American Chemical Society (ACS)).

involves three main key factors which have to be carefully characterized in the development of blood pool and/or targeted contrast agents: (i) the first one concerns the stabilization of AuNPs suspensions in bulk media (as discussed above in section 2.1.1), and it is generally taken as a part of the AuNPs synthesis step. (ii) The second one involved in the AuNPs coating involves the fabrication of nanoparticles with good *in vivo* stability and optimum *in vivo* pharmacokinetics properties, i.e. with reliable stealth properties in bloodstream. This is one of the main objective of the studies carried out for the fabrication of BPCA, and it is generally achieved with PEG-coatings which offer very poor interactions with plasma proteins.[10,11] (iii) Finally, the last factor in the AuNPs coating, which is very closely linked to the latter point (ii), concerns the surface modification in order to promote the site-specific targeting like tumor cells targeting, the so-called "active targeting". Overall, three different markers overexpressed in cancer cells are targeted by these receptor-specific functionalized nanoparticles. They are mainly matrix metalloprotease (MMPs), epidermal growth-factor receptor (EGFR), and oncoproteins that are associated with human papillomavirus (HPV) infection.[98] This AuNPs surface functionalization is summarized and illustrated in **Figure 4**, which clearly shows their potentials in terms of surface coating as well as nano-encapsulation reported in literature.

The *in vivo* imaging applications of AuNPs, with some interesting *in vitro* results have been summarized in **Table 1** and **2**.

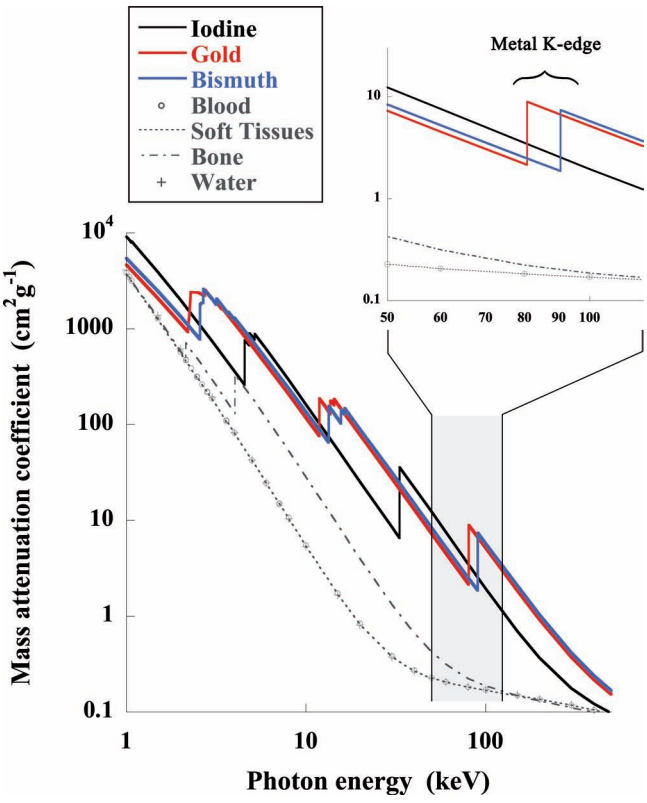

Figure 3. Mass attenuation *vs.* photon energy, of iodine, gold and bismuth, compared to blood, soft tissues, bones, and water. The energy range typically chosen for micro computed tomography is emphasized in gray (Constructed using data from Ref [87]).

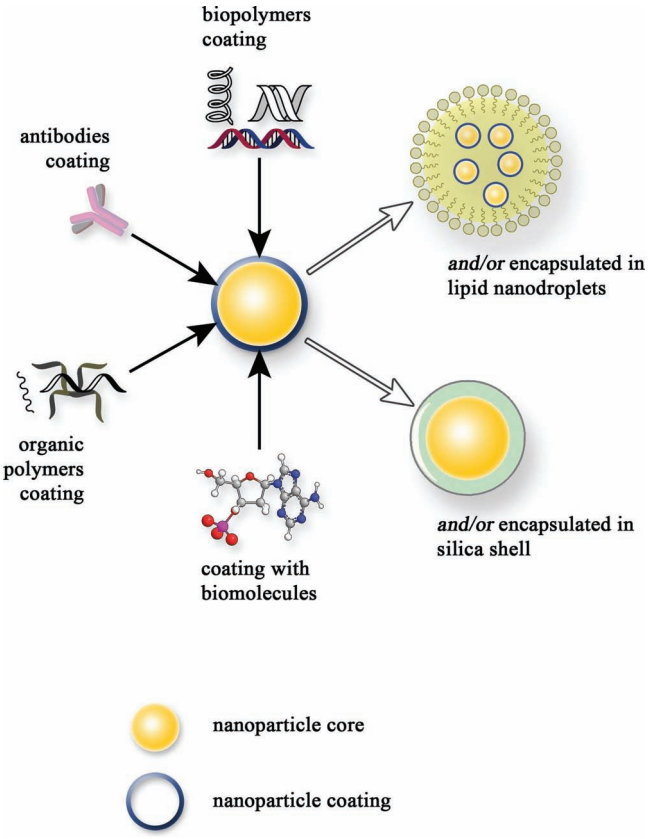

Figure 4. Schematic of surface functionalization and morphologies of inorganic nanoparticles.

We have mainly emphasized on the synthesis protocol, the coating or targeted agents specifically used either for stabilizing/surface modification of AuNPs (fundamental for *in vivo* imaging), or for active targeting of tumor cells, and finally the main application(s) and the result(s) obtained. This overview has been presented through Table 1 and there are several key fundamental points that needs to be addressed: (i) first, the citrate reduction is still one of the most important and popular methods used for AuNPs core synthesis as this method remains the easiest way to generate a stable dispersion in *aqueous media* besides surface coating of citrate can also be easily replaced by other functional molecules. However, for dendrimer entrapped gold nanoparticles, the gold synthesis follows a specific method, which plays with the particular affinities of gold ions towards the dendrimers core, followed by reduction by $NaBH_4$ (described in section 2.1.1). (ii) The second point is that the best *in vivo* stability in blood stream is given by PEGylation of AuNPs, either for BPCA applications,[10,11] or for active targeting applications (also needing a long vascular circulation).[13,14] In absence of PEG coating, the reticuloendothelial system (RES) uptake results in accumulation of AuNPs in liver and spleen. Actually, in this case (without PEG coating), there are no specific rules that can be defined to predict the in vivo stability of these systems, besides it is also influenced by other specific ligands used for targeting. (iii) The last important point is the global success of targeted CT contrast agents with AuNPs, from long circulation vascular contrast to targeted tumor cells. These results open new doors and important applications in biomedical targeted imaging, along with new possibilities for carrying out personalized cancer therapies, enabling the "online" monitoring of drug delivery *via* following-up in real time the nanocarriers imaging. The illustration of the different applications of *in vivo* imaging applications (*i.e.* BPCA, tumor active targeting, lymph nodes targeting, multimodal imaging and liver-specific imaging) are also reported from literatures, in **Figure 5**.

2.1.4. Gold nanoparticles: summary and perspectives

Over the past 5 years, the number of publications on nanoparticulate contrasts agent for CT has increased exponentially.[109] These nanomaterials assembly in function of the chemical nature of the coating layer and/or functionalization, can behave as blood pool or targeted contrast agent. Actually, the recent works in this field are mostly based on gold nanoparticles or their hybrids due to the strong X-ray attenuation of gold combined with the well-established facile chemistry of the gold nanoparticles. To date, the most significant results on long-circulating or targeted nanoparticles CT contrast agents are provided with systems based on gold nanoparticles, and summarized reported in Table 1

Table 1. Summary of the main results regarding the use of AuNPs as X-ray contrat agent, emphasizing their applications for *in vivo* imaging and/or targeting.

References	AuNPs Synthesis	Stability coating	Active targeting	Application	Main results
[10](*a*),[11](*b*)	Citrate reduction	PEG coating (incubation of	–	Blood pool	• (*a*) $t_{1/2}$ ~ 12 h; (*b*) $t_{1/2}$ ~ 14.5 h
	AuNPs, *d* = (*a*) 31 nm,	AuNPs with (*a*) PEG-SH, or		contrast agent (i.v.)	• X-ray attenuation: (*a*) 1.9 and (*b*) 2.7 times higher than Ultravist
	(*b*) 38 nm	(*b*) PEG sulfhydryl)			• Biocompatible, low toxicity, RES uptake
[88]	Commercial product	Heparin coating (conjugating	–	Liver-specific	• Liver-specific contrast
	AuNPs, *d* = 55 nm	Heparin-DOPA + AuNPs)		contrast agent (i.v.)	• Stable, biocompatible
[90]	$NaAuCl_4$ reduction by THPAL	Gum Arabic coating during the	–	Liver/lung-specific	• Enhanced contrast in juvenile swine
	(phosphino animoacid)	AuNPs synthesis, see also [99, 100]		contrast agent (i.v.)	• Good tolerance to administration
	AuNPs, *d* = 20 nm				
[12]	• Citrate reduction (17 to 66 nm)	2-mercaptosuccinic acid (MSA)	–	Spleen-specific	• Multi-color nanotags combining
	• Seed-growth method (80 to 120 nm)			contrast agent (i.v.)	surface-enhanced Raman spectroscopy (SERS) and CT
					• Dual *in vivo* imaging
[72]	Dendrimer *in situ* $HAuCl_4$	Neutral acetylated surface	–	Cancer cell imaging	• Stable in suspension for months
	reduction by $NaBH_4$, *d* = 2.6 nm			(i.t. and i.p.)	• AuDENPs accumulation in cancer cells *in vitro* and *in vivo*
[13]	Citrate reduction	PEG-COOH coating	Antibody: monoclonal	Lymph nodes targeting	• X-ray contrast enhanced in lymph nodes with targeted AuNPs
	AuNPs, *d* = 28 or 38 nm	(incubation with heterofunctional	anti-mouse CD4	and imaging (i.v.)	• Contrast enhancement stronger with bigger AuNPs
		ligand: dithiol-PEG-COOH)			
[91]	$NaAuCl_4$ reduction by THPAL	Starch coating during the	Peptide: bombesin (BBN), to	Human prostate tumor	• BBN-AuNPs specifically targets cancer receptors sites
	(phosphino animoacid)	AuNPs synthesis, see also[99]	target the gastrin-releasing	targeting and imaging	• Importance of the BBN-AuNP size for effective tumor penetration
	AuNPs, *d* = 115–150 nm		peptides (GRP) receptors	(i.p.)	
[14]	Citrate reduction	PEG-COOH coating	Antibody: anti-Her2	Human breast tumor	• Specific tumor targeting of herceptin-targeted AuNPs
	AuNPs, *d* = 15 nm	(incubation with heterofunctional	(herceptin)	targeting and imaging	• Imaging readily enables detection of small, 1.5 mm-thick tumors
		ligand: thiol-PEG-COOH)		(i.v.)	• Contrast 22-fold higher in tumors than surronding muscle

and Table 2. This simply means that, today, the best compromise between contrasting properties, physicochemical and surface properties, and low toxicity, is found with gold nanoparticles-based systems. However, these systems can reach certain limitations regarding the different aspects, and mainly the future research challenges should be focused on these points.

The first one lies in the cost of gold, which can become a critical point when the bridge between fundamental research and industrial transposition will be considered. This is actually one of the main reasons that allowed the monopole of iodinated molecules for X-ray contrast agents. The solution for getting round this problem can be found on many emerging research works focused on inorganic nanoparticles made of metal cheaper than gold, but still with X-ray attenuation properties comparable to the ones of gold. These works report that the chemistry of inorganic nanoparticles (other than gold nanoparticles) can allow realistic alternatives for the fabrication of CT contrast agents. This aspect is as well developed in detail in the second part of the present review.

Table 2. Summary of the main results regarding the use of AuNPs as X-ray contrat agent, and their applications for *in vitro* imaging and/or targeting.

References	AuNPs Synthesis	Stability coating	Active targeting	Application	Main results
[8]	Gold NanoRod (AuNR) by mediated growth method size: $d = 15$ nm, $l = 45$ nm	Poly(acrylic acid) (PAA) coating (AuNR surface adsorption)	Antibody: UM-A9 (amidation reaction on EDC/NHS activated sites)	Squamous cell carcinoma targeting and imaging ($\alpha 6\beta 4$ integrin)	• Strong selective X-ray attenuation of squamous cell carcinoma • CT imaging allows reliable and sensitive detection of lymph nodes and metastasis, in head and neck cancer diagnosis and staging
[15]	Citrate reduction AuNPs, $d = 15$ nm	–	Aptamer: prostate-specific membrane antigen RNA aptamer (PSMA)	Prostate cancer cells imaging, targeting, and drug delivery	• Strong selective X-ray attenuation of prostate cancer cells • Simultaneous and specific pancreas cancer cell targeting, imaging, and drug (doxorubicin) delivery
[16]	Citrate reduction AuNPs, $d = 15$ and 40 nm	Poly-vynil alcohol coating (added while removing citrate ions by ion exchange resin)	L-glutamic acid (primary amine for binding to the gold surface)	Damaged bone tissues targeting and imaging (-COOH chelates Ca^{2+})	• Functionalized AuNPs target damaged bones *in vitro*
[73]	$NaBH_4$ reduction AuNPs, $d = 3.2$ nm	Dendrimer G5-NH_2	Folic acid and FITC	Cancer cell targeting and imaging	• Efficiency in targeting (and thus imaging) KB cells overexpressing folate receptors
[101]	Citrate reduction AuNPs, $d = 10$–20 nm	Citrate	Thioglycolic acid, 6-thioganine, 2-mercaptoethanol, 1-propane thiol	Tracking digestive mechanisms in mosquito	• AuNPs serve as tracer in microparticles • Imaging delicate insects like mosquito
[102]	Burst synthesis $NaBH_4$ reduction $d = 6.6$–12 nm	Alkane thiolate	w-carboxylic acid	Size related attenuation properties	• Attenuation increase with decrease in size from 12 to 6.6 nm • Highly stable, monodisperse, water soluble
[103,104]	Citrate redustion $d = 4$ nm	citrate	2-deoxy-D-glucose	Cancer cell targeting and imaging	• Labelling AuNPs with 2-deoxy-D-glucose induces specific cancer cells uptake (human alveolar epithelial cancer cell line, A-549)
[105]	Various methods $d = 4$–60 nm	• 4–20 nm: citrate • 4 –20 nm: mercapto-succinic acid	–	Size related attenuation properties	• Stable in physiological conditions, nontoxic to Hela S3 cells • Higher attenuation displayed by smaller particles
[106]	Commercial product $d = 5$, 10, 20, 30, 40, 50 nm	–	–	Effect of size, concentration incubation time on the AuNPs uptake by pancreas cancer cells	• Passive cancer cell uptake depends on the AuNPs size • Better uptake with 20 nm AuNPs
[107]	Citrate reduction AuNPs, $d = 50$ nm	Horse serum protein	–	Cell imaging	• AuNPs is used a permanent marker for implanted normal and malignant cells • Quantification of cells numbers within small animals

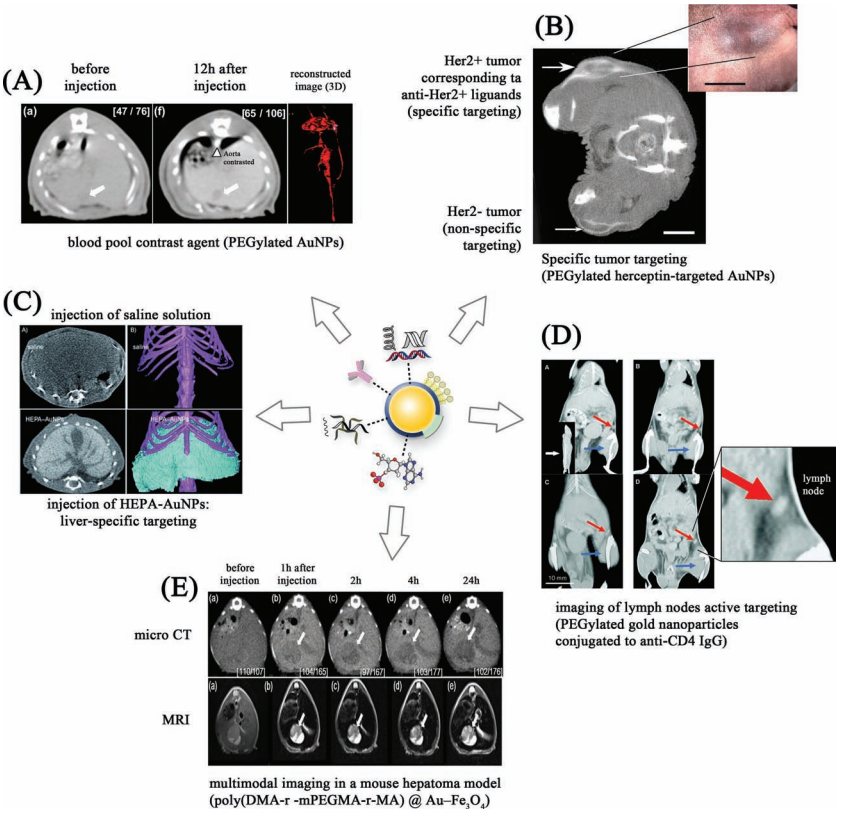

Figure 5. Schematic of the main applications of *in vivo* imaging using nano-gold. (A) Reproduced with permission.[10] Copyright 2007, American Chemical Society (ACS); (B) Reproduced with permission.[14] Copyright 2011, The British Institute of Radiology Publications; (C) Reproduced with permission.[88] (D) Reproduced with permission.[13] Copyright 2010. American Chemical Society (ACS); (E) Reproduced with permission.[108] Copyright 2011, IOP Publishing.

Gold nanoparticles and more generally of inorganic nanoparticles can appear efficient in imaging and targeted imaging. However, and it is the second limitation of these systems, their intrinsic morphology is not very adapted for their use as drug carrier, (*i.e.* for the simultaneous imaging and drug delivery). This point could actually become a predominant research interest in the near future, enabling the so-called personalized therapy. This will allow an "in time" *in vivo* quantification of the administrated drugs and a precise monitoring and control of the dosages. Earlier works of Kim *et al.*[15] (see also Table 1) already exist, in which an anticancer molecule (doxorubicin) is entrapped in the gold nanoparticle coating layer. Other potential ideas for exploring this way should lie in the multiple encapsulation of inorganic nanoparticles, for example in nanoemulsions giving possible the co-encapsulation of bioactive molecules in oil along with the contrasting NPs.

2.2. Hybrid Gold Nanoparticles

As discussed in the above section, the employment of gold in CT imaging offers unique advantages over traditional iodine based contrasting agents. Additionally their surface can be modified and functionalized with various functional materials to create new hybrid systems for use in multimodality diagnostic imaging and therapy. We will see in this section that how various coating and/or synthesis technologies associated with AuNPs allows the fabrication of hybrid gold nanoparticles that can be detected with multiple techniques such as magnetic resonance imaging (MRI), X-ray computed tomography (CT), Fluorescence imaging. Such systems can offer excellent advantages for molecular diagnosis, multimodal imaging and biotechnology. It is quite interesting to note that most of CT scanners are generally coupled with other instruments as no single imaging modality can address all biological questions. A good example could be coupling the X-ray imaging system with other imaging modalities (PET/SPECT, radionuclides etc.) which increases experimental and therapeutic flexibility. Such a combination is often used to visualize the bones with CT, in order to situate the radiolabelled probes in the whole animal body.[110–112] Such multimodal applications often allow faster detection and increases therapeutic efficacy to save time and money, but do not actually correspond to the multimodal imaging in the same line that the one discussed in the present paper, that is using multimodal NPs including CT contrast agent. Recently Wang group successfully used ^{125}I for radiolabeling of gold nanorods.[111] These probes could be successfully used as nuclear and optical dual-modality contrast agents for better examination of inflammation.

2.2.1. Gold/Gadolinium Hybrid Nanoparticles

Gadolinium, occupying central position in the lanthanide series has 7 unpaired electrons and gives excellent signal in MRI. As such coupling of AuNPs with Gd chelates can give rise to nanosystems detectable both by X-Ray CT and MRI. Roux and his group[113] were the first to develop a method to synthesize such nanosystems. They encapsulate gold nanoparticles with a multilayered organic shell composed of gadolinium chelates bound to each other with disulfide bonds (illustrated in **Figure 6** (A)). This nanoparticle complex could be served both as X-ray and MRI contrasting agent due to presence of radiopaque gold and superparamagnetic gadolinium ions. The synthetic procedure involved the reduction of gold salt in presence of dithiolated derivatives of diethylenetriaminepentaacetic acid followed by addition of Gd^{3+}. The two thiol groups played the key role in the formation of multilayered ligand shell through disulfide linkages. The *in vivo* experiments revealed free circulation of these particles in blood stream with no undesirable side effects, toxicity or accumulation in liver, lungs and spleen. These particles could be easily be detected and followed up by MRI and X-ray imaging despite of low concentration of gold (10 mg/mL) and gadolinium (5 mg/mL). Various other research groups also reported the functionalization of AuNPs with Gd DTPA

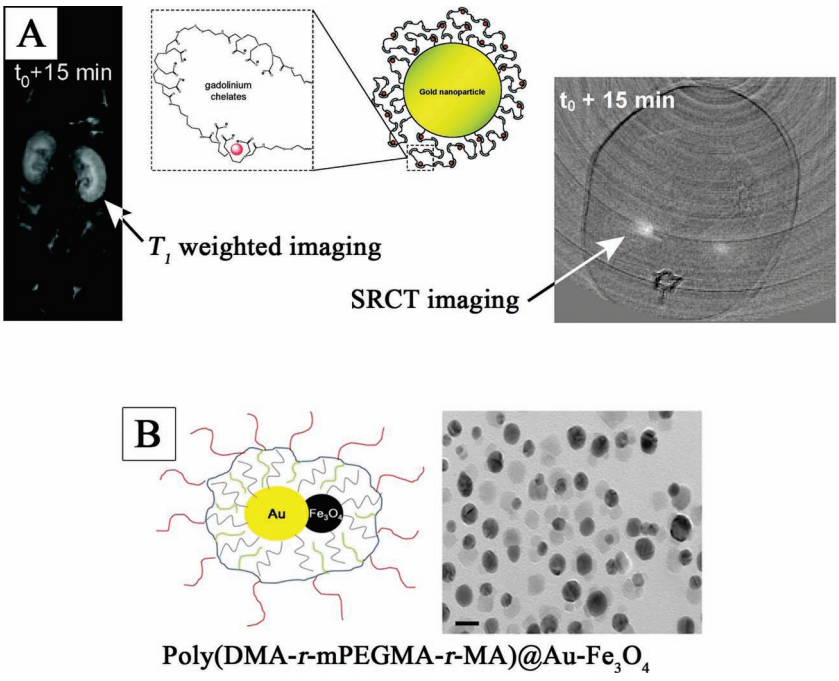

Figure 6. Gold-based nanoparticles for multimodal imaging: (A) Gold-gadolinuim chelate for X-ray and MRI imaging (Reproduced with permission.[113] Copyright 2008. American Chemical Society (ACS); (B) Hybrid gold/iron oxide for dual CT/MRI imaging, corresponding to the images reported in Figure 5 (E) (Reproduced with permission.[108] Copyright 2011, IOP Publishing).

complex using conjugates like penicillamine,[114] 4-aminothiophenol[115] and cysteine.[116] These particles exhibited very high r_1 and r_2 relaxivity. The *in vivo* X-ray attenuation of these conjugate particles[114] was found to be almost twice as compared to simple ligand coated gold particles and displayed excellent contrast enhancement of liver, the blood pool and lymph nodes with no visual side effects. In a similar approach Song *et al.*[117] used oligonucleotide-modified gold nanoparticle conjugates for covalently attaching GdIII complexes (DNAGdIII@AuNP). This nanoparticle conjugate was highly biocompatible and stable with an extraordinary ability to enter cells, which were about 50 folds higher as compared to the clinically available contrast agent DOTAGdIII. This nanoparticle system was suitable for CT and MRI applications and could also be used in fluorescence imaging by attachment of fluoroprobes like Cy3 (cyanine dye) to the DNA strand.

2.2.2. Gold/Iron Oxide Nanoparticles

Similar nanosystems active both in MRI and CT imaging can also be designed by using superparamagnetic iron oxide with AuNPs. Jon and coworkers studied two types of systems containing both iron and gold.[108,118] The first one published in 2009 reported polyethylene glycol (PEG) coated hybrid core-shell type nanoparticles consisting of iron oxide core and gold shell. The synthesis protocol involved deposition of gold layer over superparamagnetic iron oxide core particles coated with oleyamine. The surfaces of the particles were coated with a layer of PEG to ensure biocompatibility and long circulation time in blood stream even at high concentration. The X-ray contrasting effect was found to be higher when compared with iodinated contrasting agents. Recently, they developed hybrid nano-emulsions containing both gold and iron oxide[108] (illustrated in Figure 6 (B) and Figure 5 (E)). This nanoemulsion was synthesized by thermal decomposition of Fe-oleate and Au-oleylamine complexes and were coated with amphiphilic poly(DMA-r-mPEGMA-r-MA) to prevent their aggregation and make them water soluble. The particles displayed high contrast in CT imaging which was even more than pure gold nanoparticles. The *in vivo* experiments with hepatoma"bearing mice resulted in high contrast difference between hepatoma and normal tissue in liver.

2.2.3. Gold/Silica Nanoparticles

Another approach for the development of multifunctional probes for MRI, CT and fluorescence imaging was shown by Mulder and co-workers.[119] In their experiments they deposited a fluorescent and paramagnetic lipid coating (contaning Cy5.5 (NIR dye) and a Gd conjugate) over gold/silica core shell-type nanoparticles. This system exhibited magnetic and optical properties with the dense gold core serving as X-ray contrast agent. The PEGylated layer was essential to ensure a water dispersible, stable and biocompatible system. The CT or MRI contrast per particle could easily be tuned by increasing or decreasing the surface area simply by manipulating the size of gold core. This system was highly sensitive and it was possible to get *in vivo* signal enhancements in mice liver by 24% and 50% for MRI and CT, with concentration as low as 0.15 nmol·kg^{-1}. In their another study, they modified high density lipoproteins (HDL) by replacing their hydrophobic core with gold, iron oxide or quantum dot nanoparticles[120] (see **Figure 7**). The authors used ordinary phospholipid, gadolinium

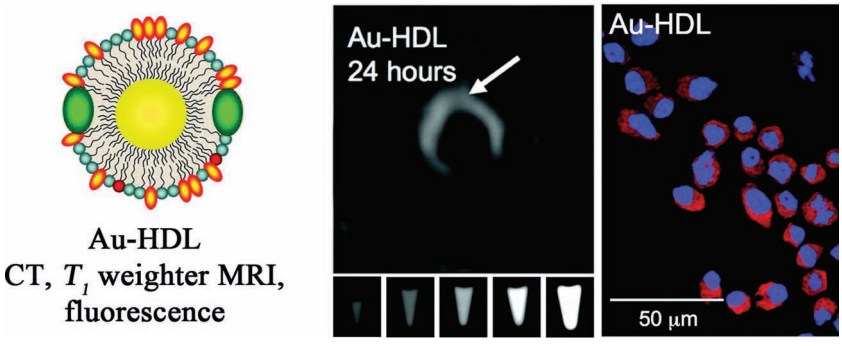

Figure 7. Lipid coated gold nanoparticle for multimodal CT/MRI/fluorescence imaging (Reproduced with permission.[120] Copyright 2008, American Chemical Society (ACS)).

labeled phospholipid and rhodamine labeled phospholipids to synthesize these nanocrystal core HDL. This system was not only multimodal but it was seen that the gold core based nanosystems displayed more contrast than Omnipaque and PEG coated gold nanoparticles. The *in vitro* experiments demonstrated the uptake of nanoparticles by macrophages. This nanosystem could also be specifically targeted for imaging of atherosclerosis when *in vivo* experiments were performed with mice fed exclusively with cholesterol rich diet.

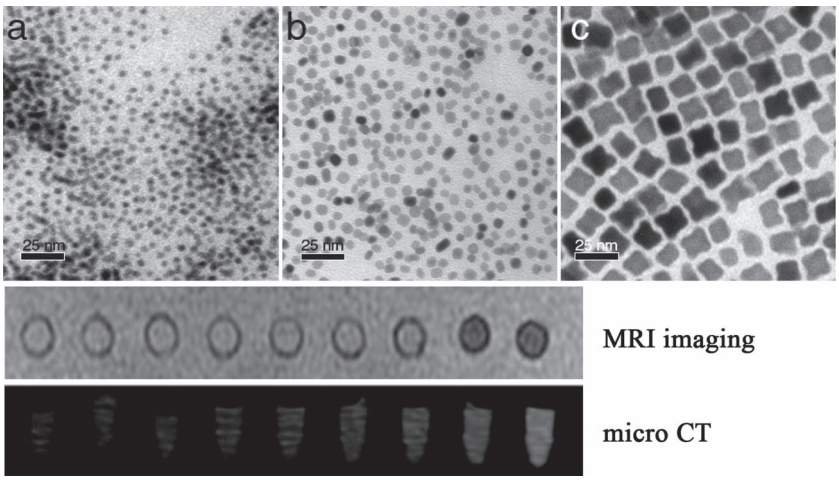

Figure 8. Hybrid FePt nanoparticles for multimodal MRI/CT imaging (Reproduced with permission.[134] Copyright 2010, American Chemical Society (ACS)).

2.3. Silver Nanoparticles

Colloidal form of silver compounds like AgI and Ag_2O[121–126] were used as contrast materials in the earlier 20th century but their use were quickly abolished because of the high toxicity and fatalities encountered.[127,128] However, studies on silver iodide colloids way back in the late seventies revealed that silver was retained in the liver long enough to allow CT examination with the contrast difference of 4 to 5 times that the background.[126]

Silver nanoparticles as such suffer from the same drawback regarding toxicity issues,[129–131] but with new developments and technological advancements the toxicity of silver nanoparticles has not only been greatly reduced but they could be made more biocompatible with appropriate surface modifications.[132]

In a recent report Lui *et al.*[133] reported the X-ray contrasting properties of dendrimer stabilized silver nanoparticles which could also be used for *in vivo* CT imaging applications. They reported size controlled facile synthesis of silver nanoparticles using G5 PAMAM dendrimer (generation 5 poly(amidoamine)) as template. By simply varying the molar ratio of dendrimer/Ag salt they could easily tune the size of silver nanoparticles from 8.8 to 23.2 nm. The dendrimer templated silver nanoparticles were not only stable in water, PBS buffer, fetal bovine serum but also at different pH (pH 5-8) and temperature (20–50 °C) conditions. The X-ray absorption coefficient of silver nanoparticles was found to be both size and concentration dependent. It was found that particles with diameter of 16.1 nm displayed X-ray attenuation properties similar to that of iodine based contrasting agent (Omnipaque) even though the atomic weight of silver is lower than that of Iodine. *In vivo* experiments with mice the silver particles displayed prolonged contrast enhancement and did not showed any toxic effect.

2.4. Platinum Based Nanoparticles

Though platinum can serve as a good contrasting agent due to its high atomic number, (Z = 78) but till date only little work has been done in this respect. Recently Chen's lab demonstrated that water dispersible FePt nanoparticles[134] can potentially serve as a dual modal contrast agent for both CT and MRI molecular imaging where the heavy Pt contributed mainly as X-ray contrasting agent. These nanoparticles could easily be prepared by a simple synthetic route and the size could be tuned between 3, 6 and 12 nm by simply changing the reaction conditions. This example is reported in **Figure 8** where the TEM pictures show three different sizes of FePt particles, along with MRI and CT imaging phantoms emphasizing their contrasting properties. The particles presented excellent biocompatibility (cell viability >75% at 0.1 M) and hemocompatibility (<5%) in all imaging contrast experiments. Surface chemistry and size played a crucial role in biodistribution, half-life, X-ray contrast and target specificity. For example the 12 nm FePt nanoparticles revealed highest serum concentration, circulation half life and X-ray contrast while the 3 nm particles presented highest concentration in the brain and can be ideal for brain mapping. The nanoparticles could also be targeted to specific sites like tumor cells when conjugated with antibodies and other function ligands.

3. Heavy Metal Based Nanoparticles (Thorium, Bismuth and Tantalum)

Heavy metals are good X-ray absorbers due to their high density and atomic weight. The X-ray attenuation of heavy metals also remains more or less constant with increasing X-ray energies, a phenomenon which arises due to higher K-edge of heavy elements which falls within diagnostic X-ray spectrum. Although living organisms require varying levels of certain heavy metals, their excessive levels can be toxic and dangerous. Certain heavy metals may cause severe side effects and their accumulation over time can cause serious illness or even death.

3.1. Thorium Oxide Nanoparticles (ThO_2)

Perhaps thorium based nano-emulsions are the first that fall into this category. Colloidal thorium oxide (ThO_2) under the name Umbrathor produced by the Heyden Chemical Company was introduced in Germany as a radiological contrast agent in the late 1920s.[135] Umbrathor was a stable brownish liquid

containing 25% ThO_2, which was administrated orally for visualization of the gastrointestinal tract. Later thorium oxide solution with particle size of 3–10 nm and trade name of Thorotrast was introduced was produced by Testagar and Company.[136,137] This version of colloidal ThO_2 was alkaline-stable and did not aggregate after intravenous administration. Thorotrast was an opalescent and colorless colloidal solution of 25% colloidal ThO_2 (19–20 wt.%) and Dextrin (16–19 wt.%) with about 0.15 wt.% of p-hydroxy benzoate as a preservative.[5,137] It proved to be an ideal radiographic agent and showed excellent contrasting properties due to the high atomic weight of thorium. It could be administrated both intravenously and intra-arterially and was mainly used mainly in angiography. Later due to its excellent X-rays absorbing abilities it was used practically in every radiological contrast study and excellent images were obtained of liver, bladder, urethra, spleen, vessels etc. Other uses of Thorotrast included oral administration for imaging of gastric mucosa and upper part of gut.

Intravenous injection of Thorotrast was considered to be safe at that time as it was quite painless with little adverse effects, however after many years of research it was found that almost all of the injected Thorotrast was retained within the body and the particles were deposited lifelong in the reticuloendothelial system of many organs like liver, spleen, bone marrow and lymph nodes. The biologically half-life was also very high which was estimated to be 400 years,[138] as such once injected thorium was retained inside the body throughout the patient's life. The long term side-effects was due to the radioactive nature of Thorium in ThO_2 (half-life 1.4×10^{10} years) which caused formation of malignant tumors, liver fibrosis, blood dyscrasias, leukemia etc even after 20 years of application.[139–143] The use of colloidal ThO_2 was finally discontinued because of the high toxicity encountered.

3.2. Bismuth Based Nanoparticles

Bismuth as a heavy metal displays unusually low toxicity which makes it suitable for various medicines, cosmetics and medical procedures. Bismuth salts were one of the earliest X-ray contrast agents to be used on human patients. The first radiographic use of bismuth compounds dates back to 1897–98, when a suspension of bismuth subnitrate was used to image human gastrointestinal tract.[5,144,145] Bismuth subnitrate emulsions were also used for the contrast enhancements in coronary angiogram. However due to high cost and toxicity associated with high doses of bismuth compounds resulted their discontinuation and they were replaced by cheaper alternatives.[5]

In 2006 Weissleder group reported polymer-coated Bi_2S_3 nanoparticles (BPNPs) as a new injectable contrast agent for CT imaging.[146] The nanoparticles were initially grown by refining an earlier method, followed by their surface modification by a biocompatible polymer poly(vinylpyrrolidone). The resulting nanoparticles were flat, rectangular platelet shaped of size range of 10–50 nm and 3–4 nm in thickness. Coating with PVP was an essential step as it rendered the nanocrystals biocompatible, highly soluble in water, more inert and increased their half-life when administrated intravenously. The X-ray opacity of these nanoparticles was found to be 5 fold higher

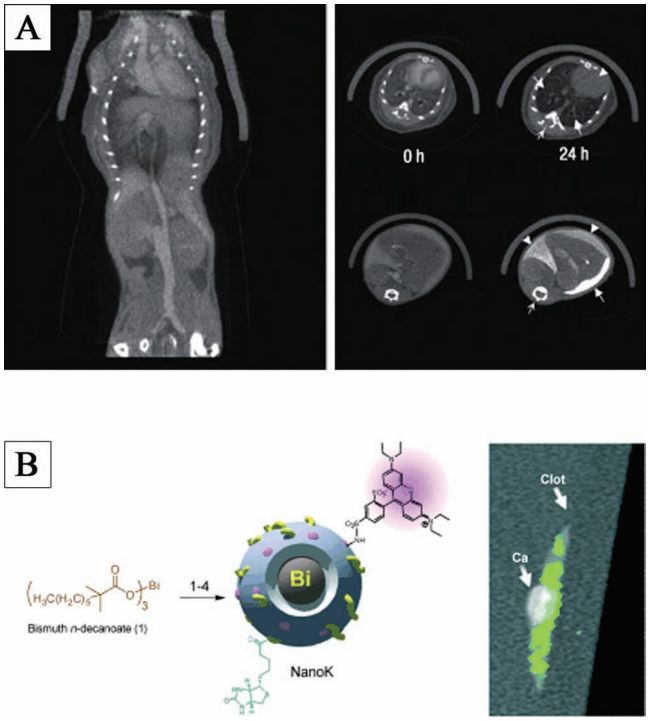

Figure 9. Bismuth-based nanoparticles for CT imaging. (A) BPCA made with bismuth sulphide nanoparticles (Reproduced with permission.[146] Copyright 2006, Nature Publishing Group); (B) Multimodal and clot imaging. Reproduced with permission.[148]

than that of commercial available iodine based contrasting agent and thus much lower doses can be used to produce same contrast. Preliminary *in vivo* experiments with mice showed that the nanoparticles were retained in the bloodstream far longer than commercial iodine based contrasting agents. This example is reported in **Figure 9** (A), showing (left) the whole mouse body with contrast vasculature, and (right) temporal evolution from the blood (after injection) and accumulation in liver and spleen (24h after injection). An increase in signal in the reticuloendothelial system was also observed when delayed imaging experiments were carried out at 12–24 h after intravenous administration. Initial cytotoxicity assay showed bismuth sulfide nanoparticles to be less toxic than even commercial iodine based contrasting agent (Iopromide) and substantial lower toxicity than Bi^{3+} salt. In the same year another report was published where radiopaque bismuth and barium sulfate based micro capsules were used for X-ray guided delivery and imaging of cellular therapeutics.[147] The radiopaque material was added to the inner core layer surrounded with a layer of alginate-poly-L-lysine-alginate (APA) from outside to avoid any toxic effects. The *in vivo* results with mice and rabbit demonstrated that the microcapsules could even be visualized singly. They also possessed long lasting contrast properties (two weeks), most probably due to low water solubility.

In a recent report also bismuth enriched nanocolloides were used as contrasting agents to detect clots and make them visible by using a rather new technique, spectral CT molecular

imaging[148] (see Figure 9 (B)). Spectral CT imaging aims to enhance traditional CT diagnostic capability and can quantify certain elements based on their distinctive K-edge energies. Pan and his group designed a special bismuth based nanocolloid which contained a core made up of bismuth atoms attached to n-decanoic acid suspended in sorbitan sesquioleate (a mixture of fatty acids) and encapsulated in a phospholipid membrane. The electrophoretic potential of these nanocolloids ranged from −20 to −27 mV and the hydrodynamic diameter was around 180 and 250 nm. These nanoparticles were so designed that they reduced the toxicity of bismuth by releasing the inner bismuth compound in a safe non-toxic form. These nanoparticles were capable of interacting and combining with the fibrin protein found in blood clot and showed excellent signal enhancement of the clot. The heavy metal bismuth was found to be bioeliminated from the body within two weeks of intravenous administration.

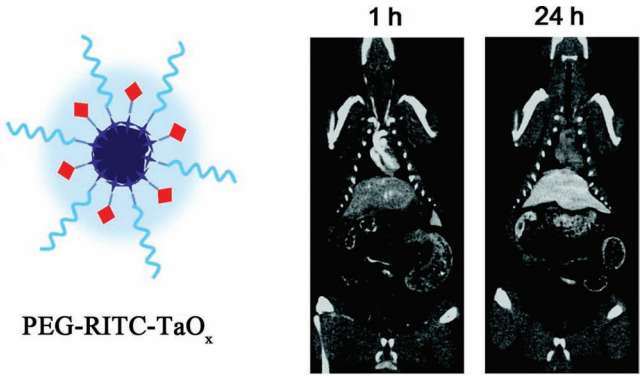

Figure 10. Tantalum based nanoparticles for multimodal CT imaging, BPCA and lymph nodes imaging (Reproduced with permission.[157] Copyright 2011, American Chemical Society (ACS)).

3.3. Tantalum Based Nanoparticles

Ongoing and previous researches have placed Tantalum as one of the potential X-ray contrasting agents as it has shown some advantages over traditional iodinated contrasting agents. Tantalum metal is highly radiopaque and has a high atomic weight with density of 16.6 g/mL, as such only a small amount is sufficient enough to product sufficient contrasting effect. Tantalum powder was first used as contrasting agent for bronchography in the early 1970s.[149–152] Later Tantalum oxide Ta_2O_5 powder which is a biocompatible and an inert oxide with high radiopacity was also tested for similar studies and excellent results were obtained. Other studies showed that tantalum could also be used for gastro-intestinal imaging and angiography.[153–155]

Water soluble tantalum oxide nanoparticles with particle size less than 6 nm were recently investigated for their contrasting properties by Bonitatibus *et al.*[156] The particles were formulated in form of core-shell type structure which could be administrated intravenously. The synthesis of nanoparticles was a two-step process, which involved the synthesis of tantalum oxide core by controlled hydrolysis of tantalum ethoxide followed by coating with a silica shell. The silica shell imparted high water solubility and high stability to the cores, and the concentrated aqueous solutions of these particles remained stable for about 6 months without any change in size. The *in vitro* studies of these nanoparticles indicated superior contrast as compared to iodine. Experiments performed at high X-ray energy showed more or less a constant contrast effect for tantalum as compared to that iodine where contrast decreased with increasing X-ray energy. The *in vivo* studies in mice showed no acute or toxic effects as such and displayed subsequent renal clearance. Recently Hyeon and coworkers used a microemulsion method for the synthesis of uniform size TaO_x particles in gram scale quantities[157] (illustrated in **Figure 10**). The surface of these particles could easily be functionalized with silane derivatives by a simple *in situ* sol-gel reaction. This step was necessary as these derivatives provided antifouling and biocompatible properties. This surface modification also provided a platform for attachment of functional molecules like PEG and fluorescent dyes. This induced fluorescence as well as increased the *in vivo* circulation time (see the vascular contrast 1h after injection in Figure 10), making them suitable for image-guided lymph node mapping and CT angiography. The *in vivo* toxicity studies revealed no adverse toxicity on normal function of organs.

The high radiopacity, hardness, inertness and transparency of tantalum oxide makes it a promising material for dental filling.[158–162] Radiopacity is a desired feature for most of the dental materials for diagnostic purposes and X-ray detection of the filler. Researches by various groups have shown that surface functionalized tantalum oxide nanoparticles can serve this purpose well. For example Rawls research group synthesized and studied the properties of biocompatible phosphate methacrylate functionalized Ta_2O_5 nanoparticles and coupled it with a matrix monomer.[158] Their studies showed that these nanoparticles can act as non-associated radiopaque component of the resin composite used for dental filler. Similarly Schulz *et al.*[160] used flame spray pyrolysis method for the controlled synthesis of 6–14 nm Ta_2O_5/SiO_2 nanocomposites with specific properties. The synthesis involved flame spray pyrolysis of a precursor solution (*e.g.* Ta butoxide and tetraethoxysilane) using hexane as a solvent. They found out that the properties (refractive index, transparency etc.) of the final product could be easily manipulated and controlled by changing the ratio of the Ta and Si precursor. The benefits of this mixed nanocomposite as a dental filler was its high transparency in the visible spectrum, broad range of refractive index and radiopacity.

4. Rare Earth Nanoparticles

4.1. Gadolinium Based Nanoparticles

The high atomic weight and large number of unpaired electron makes Gadolinium an excellent contrasting agent both for MRI and CT imaging. The K-edge (52 keV) of Gd is higher than iodine and thus produces a greater attenuation of X-rays and better contrast than iodine. Gadolinium oxide suspensions were first tested as contrasting agents for X-ray CT imaging in the late 70's by Havoron *et al.*[126,163] They found out that

polyvinylpyrrolidone stabilized Gd_2O_3 microparticles displayed excellent contrasting properties with no observable toxic effects in laboratory animals.

Recently Prosser group[164] developed a two-step route for the synthesis of poly(acrylic acid) stabilized lanthanide fluoride nanoparticle aggregates. The nanoparticle aggregates consisting of either $NaGdF_4$ or a 50/50 mixture of GdF_3 and CeF_3 were tested for their applications in MRI and CT imaging. A low polydispersity was observed for the particles and their size could easily be manipulated by varying ratio of Gd^{3+} and Ce^{3+}. X-ray diffraction and high resolution STEM studies confirmed that the aggregates were in fact made up of smaller particles with an average size of 20–22 nm in case of $NaGdF_4$ and 10–12 nm in case 50/50 mixture of GdF_3 and CeF_3. They displayed high relaxivities at 1.5 and 3 Tesla ($35-40\ s^{-1}\cdot mg^{-1}\cdot mL$) in MRI which was much higher than Gd^{3+}-DTPA complex. For CT measurements their X-ray attenuation were compared with Gd^{3+}-DTPA and iopromide at different X-ray energies (25, 35, 45 and 49 keV). It was found that the nanoaggregates displayed higher attenuation at energies below 30 keV and above 50 keV when compared with iopromide and also outperformed Gd^{3+}-DTPA complex at all X-ray energies. Further the aggregates could also be made target specific to human cancer cells by functionalizing PAA with folic acid.

In another study Watkin's group reported the development of Gd_2O_3 nanoparticles[165,166] of diameter of 20–40 nm embedded within protein microspheres which displayed multimodal contrast for MRI, CT and US imaging. The formulations of these microspheres were rather simple, Gd_2O_3 nanoparticles were simply dispersed in oil followed by addition of filtered aqueous solution of 5% bovine serum albumen in 1:1:10 concentration ratio. The mixture was then heated to 55 degrees C followed by ultrasonic irradiation, washing and resolubilization in distilled water. The CT attenuation of Gd_2O_3-Albumin microspheres was found to increase linearly with concentration and was found to be 40 to 100 times higher than iopamidol on equimolar basis. In another similar approach Santra group designed and engineered single-core-multiple-shell Ru(bpy):Gd*III*/ SiO_2 nanoparticles through a one pot synthesis route for use as multipurpose imaging probes (Ru(bpy) = tris(2,2′-bipyridyl) dichlororuthenium(II) hexahydrate).[167] The nanoparticles were photostable, radiopaque, paramagnetic and were active as contrasting agent for MRI, CT imaging and diffuse optical tomography. They consisted of a silica core doped with organometallic photostable Ru(bpy) dye, surrounded by a inner hydrated silica shell consisting of paramagnetic gadolinium (III) ions, attached to silica shell *via* silane ligands. The core isolated the Ru(bpy) dye molecules and prevented its photo bleaching from outside environment without causing any change in the fluorescence characteristics. Both the heavy electron dense metal ions contributed towards the radiopacity and displayed X-ray contrast. The outermost silica shell consisted of surface reactive groups which could be specially modified by amine groups, ligands or antibodies for specific targeting and *in vivo* experiments. The composite nanoparticles exhibited strong fluorescence at 600 nm and were found to generate MR contrast for both longitudinal (T1) and transverse (T2) proton relaxation rate measurements which was higher than the commercially available Gd-HP-DO3A contrasting agent. They also displayed radiopacity, although they were less contrasting than commercially available Omnipaque®at equal concentration.

4.2. Holmium Nanoparticles

Similar to gadolinium, holmium also shows multimodal contrasting behavior and serves as excellent contrasting agents both for MRI and CT imaging due to its paramagnetic nature and high atomic number. Recently studies by Nijsen group have shown that holmium displays more CT contrast than commonly used iodine based contrasting agents.[168,169] The group synthesized both micro and nanosized particles of HoAcAc and studied their contrasting properties for both MRI and CT imaging. In case of holmium microspheres it was seen that they had higher holmium content than the starting material which increased their sensitivity for MRI and CT imaging.[168] The mass attenuation coefficient of these microspheres at 120 keV was found to be 15.6 $HU\cdot mg^{-1}$ which was found to be higher than that of iodine based contrasting agent. The group also studied spherical HoAcAc nanoparticles with diameters about 200 folds lesser than microparticles.[169] The nanoparticles were stabilized by PVA (polyvinyl alcohol) or DMAB (didodecyldimethylammonium bromide) and synthesized using a solvent evaporation process. They were similar to microspheres and were contrasting in both MRI and CT imaging. The average particle size was 78 nm in diameter and were quite stable in buffer solution. It was seen that nanoparticles had a clear advantage over microparticles as their small size and positive surface zeta potential prevented their aggregation prior to administration.

5. Soft X-ray molecular probes

Soft X-ray molecular probes are materials which are good absorbers of soft X-rays. Elements with mid-range atomic number fall in such category. Two such examples studied are Pd and TiO_2 nanoparticles which were found to be good soft X-ray contrasting agents.

5.1. Palladium Nanoparticles

Palladium can be used as contrast enhancer when used with as X-ray beam of lower energy due to the lower energy of k-edge absorption peak of Pd (24.35 keV) which is situated close to the mean energy of X-rays. The contrasting effect in CT imaging of biomolecule stabilized palladium nanoparticles were studied by Kannan and collaborators.[170] For biocompatibility Pd nanoparticles were synthesized strictly in a non-toxic environment. To achive this, first palladium ions were reduced by non-toxic reducing agents (trishydroxyphosphine alanine "Katti's Peptide", THPAL) in presence of biocompatible biomolecules like gum arabic and gelatin to stabilize the particles. Here gum arabic or gelatin played the role of stabilizing agent and also to render the nanoparticles suitable for bio environment. They observed that the change of CT number (HU) with concentration in case of palladium was higher as compared to that of gold at low X-ray energies.

5.2. Titanium-dioxide Nanoparticles

TiO_2 is another soft X-ray molecular probe which can be used as a contrasting agent along with other heavy metal contrasting agents.[171] The two basic advantages of TiO_2 are that firstly they are highly biocompatible and secondly they are quite suitable as contrasting agent when used with soft X-ray imaging. Larabell group reported[171] the development of TiO_2–streptavidin nanoconjugate, a new biological label via a two-step synthesis approach where the first step involved synthesis of TiO_2 nanoparticles *via* a high temperature pyrolysis reaction using TOPO as capping agent followed by ligand exchange of TOPO with polyacrylic acid while the second step involved nano conjugation with streptavidin using a bridging molecule (1-ethyl-3-[3-dimethylaminopropyl]carbodiimide hydrochloride). The author concluded that such molecular probes can be used together with gold nanoprobles to obtain quantitative information and location of proteins using X-ray microscopy.

6. Other types

6.1. Iron oxide Nanoparticles

Iron oxide nanoparticles, best known as an excellent MRI contrast agent can also be used to increase the radiopacity of hydroxyapatite, a material commonly used for a variety of bone filling and augmentation applications. Hydroxyapatite based implants such as porous blocks and self-setting cements shows a poor contrast and as such it is not easy to monitor its implant and early diagnosis complications. In a recent publication Varma's group[172] synthesized iron oxide nanoparticle-hydroxyapatite composite by co-precipitating method using iron salt. They reported a considerable increase in contrast due to presence of iron oxide nanoparticles, besides such interaction did not interfere with physical parameters of hydroxyapatite like phase purity, grain size and morphology of hydroxyapatite. Preliminary cytotoxicity experiments were also carried out and the iron oxide-hydroxyapatite composite was found to be non-toxic with good cell activity.

6.2. Quantum Dots

CdS based quantum dots which are commonly used for fluorescence experiments due to their high quantum efficiency of fluorescence can be designed as multimodal probes for medical diagnosis. In 2005 Sandra and coworkers developed ultrasmall 3.1 nm surface modified CdS:Mn/ZnS core-shell type of quantum dots which could be used as multimodal contrast agent in MRI, CT and FI imaging.[173] These quantum dots were highly soluble in water, stable in *in vivo* environment as well as suitable for conjugation with biomolecules. A single step microemulsion method (water-in-oil) was used for synthesis of quantum dots, which were further coated with a layer of silica with amine groups. The coating of silica layer increased their solubility in water by many folds and also acted as a platform for bioconjuation with biomolecules like DNA, peptides etc.

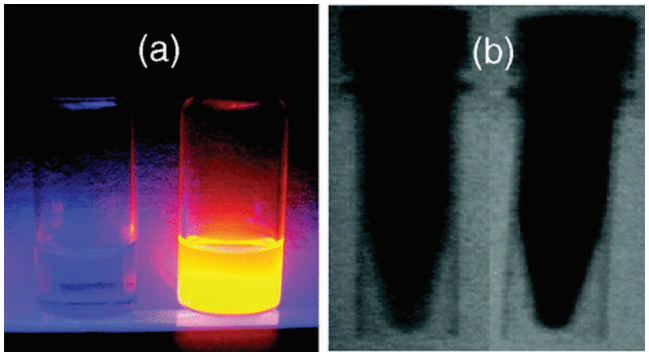

Figure 11. Quantum dots for multimodal CT/fluorescence imaging (Reproduced with permission.[173] Copyright 2005, American Chemical Society (ACS)).

The particles were, however, less radiopaque than iodine based contrasting agent like Omnipaque. This example is illustrated in **Figure 11** presenting optical and radio-opaque multimodal properties of such a nanoparticulate system.

7. Conclusions and Outlook

X-ray computed tomography (CT) is one of the most widely used techniques in scientific and technological applications. It is one of the oldest diagnostic tools in terms of frequency of use and cost, yet its use is quite limited due to the limitations faced by current clinical contrasting agents based on small iodinated molecules. The design objective of next generation contrasting agents will probably focus on materials with tissue targeting properties, long retention time and multimodal characteristics. Nanomaterials as such can play an important role in development of such contrasting agents which can provide a flexible platform for next generation contrasting agents. New applications of inorganic nanomaterials as BPCA, tumor and lymph node targeting, are being thoroughly studied. However numerous challenges need to be overcome before they are approved for clinical purposes. Besides, there is currently little experimental data on the toxicity of a vast range of available nanoparticles, which is also difficult to measure directly. These materials are still in trial phase and observations till date are only limited to in-vitro experiments or preliminary animal studies. Other drawbacks include high cost, longer retention time, and incomplete toxicity and efficacy studies.

Gold nanoparticles which have been used for centuries in many countries as traditional medicines to cure certain diseases have been recently a subject of extensive research due to their contrasting properties in the X-ray region. It is quite likely that they may be used as a commercial contrasting agent in near future. It is one of the most attractive nanomaterials which can be synthesized and purified easily and seems to have several advantages over traditional iodinated contrasting agents which include higher attenuation coefficient, inertness and biocompatibility, longer retention time, low osmolality and viscosity, effective tumor targeting (in conjugation with antibodies, peptides etc.), rapid removal from kidneys, stability at

high concentration etc. The other advantages include conjugation with gadolinium complexes, fluorescent dyes or iron nanoparticles for multimodal imaging in MRI, X-ray CT imaging and fluorescence imaging. The size of gold nanoparticles also seems to play an important role as it has been seen that gold particles of different diameters tend to diffuse and accumulate in specific organs of the body[174] besides the attenuation properties of gold nanoparticles is also related to particle diameter and is found to be higher for smaller particles.[102,105]

Other heavy elements based nanoparticles (Z>53) like Ta_2O_5, Bi_2S_3, FePt, holmium etc. have also shown interesting results in preliminary in vivo X-ray imaging experiments and can potentially better address clinical needs. Bismuth nanoparticles, for example, can serve as an alternative which can also be used for detection of dangerous blood clots. Multimodal nanoparticles like iron-platinum alloy (FePt) nanoparticles and gadolinium or holmium based nanoparticles can potentially be used as dual modal CT/MRI molecular imaging contrast agents in clinical settings.

To shift into an entirely new clinical platform however requires many precautions. Each study will require thorough examinations by preclinical trials. As discussed above, most of the inorganic nanoparticles based X-ray contrast agents are still in trial phase and there are several key issues that need direct attention. The major challenge lies in the toxicological studies which are still incomplete and uncertain as materials in the nano-regime can take on radically different properties not seen in their bulk counterparts. The cost effectiveness is also another major issue which needs to be taken into account. We, however, do believe that surface functionalization and modification will gain more attention and that increased collaboration between experts from biological and chemical sciences, medicine, and nanotechnology will yield new fundamental insights to reach the final goal.

Received: February 3, 2012
Published online: May 18, 2012

[1] H. Pietsch, U. Hbner-Steiner, P. Seidensticker, *X-Ray Contrast Media*, Wiley-VCH Verlag GmbH & Co. KGaA, **2002**.
[2] J. A. Sicard, J. Forestier, L. Laplane, *Rev. Neurol.* **1923**, *6*, 676.
[3] F. Hallouard, N. Anton, P. Choquet, A. Constantinesco, T. Vandamme, *Biomaterials* **2010**, *31*, 6249–6268.
[4] J. F. Hainfeld, D. N. Slatkin, T. M. Focella, H. M. Smilowitz, *Br. J. Radiol.* **2006**, *79*, 248–253.
[5] S. B. Yu, A. D. Watson, *Chem. Rev.* **1999**, *99*, 2353–78.
[6] M. C. Daniel, D. Astruc, *Chem. Rev.* **2004**, *104*, 293–346.
[7] J. F. Hainfeld, D. N. Slatkin, H. M. Smilowitz, *Phys. Med. Biol.* **2004**, *49*, N309–N315.
[8] R. Popovtzer, A. Agrawal, N. A. Kotov, A. Popovtzer, J. Balter, T. E. Carey, R. Kopelman, *Nano Lett.* **2008**, *8*, 4593–4596.
[9] J. Turkevitch, P. C. Stevenson, J. Hillier, *Discuss. Faraday Soc.* **1951**, *11*, 55–75.
[10] D. Kim, S. Park, J. H. Lee, Y. Y. Jeong, S. Jon, *J. Am. Chem. Soc.* **2007**, *129*, 7661–7665.
[11] Q. Y. Cai, S. H. Kim, K. S. Choi, S. Y. Kim, S. J. Byun, K. W. Kim, S. H. Park, S. K. Juhng, K. H. Yoon, *Invest. Radiol.* **2007**, *42*, 797–806.
[12] M. Xiao, J. Nyagilo, V. Arora, P. Kulkarni, D. Xu, X. Sun, D. P. Davé, *Nanotechnology* **2010**, *21*, 035101–035108.
[13] W. Eck, A. I. Nicholson, H. Zentgraf, W. Semmler, S. Bartling, *Nano Lett.* **2010**, *10*, 2318–2322.
[14] J. F. Hainfeld, M. J. O'connor, F. A. Dilmanian, D. N. Slatkin, D. J. Adams, H. M. Smilowitz, *Br. J. Radiol.* **2011**, *84*, 526–533.
[15] D. Kim, Y. Y. Jeong, S. Jon, *ACS Nano* **2010**, *4*, 3689–3696.
[16] Z. Zhang, R. D. Ross, R. K. Roeder, *Nanoscale* **2010**, *2*, 582–586.
[17] G. Frens, *Nature: Phys. Sci.* **1973**, *241*, 20–22.
[18] K. J. Watson, J. Zhu, S. B. T. Nguyen, C. A. Mirkin, *J. Am. Chem. Soc.* **1999**, *121*, 462–463.
[19] T. Yonezawa, T. Kunitake, *Colloids Surf. A: Physicochem. Eng. Asp.* **1999**, *143*, 193–199.
[20] M. Faraday, *Philos. Trans.* **1857**, *147*, 145–181.
[21] M. Brust, M. Walker, D. Bethell, D. J. Schiffrin, R. J. Whyman, *J. Chem. Soc. Chem. Commun.* **1994**, 801–802.
[22] M. Brust, J. Fink, D. Bethell, D. J. Schiffrin, C. J. Kiely, *J. Chem. Soc. Chem. Commun.* **1995**, 1655–1656.
[23] S. Chen, *Langmuir* **1999**, *15*, 7551–7557.
[24] S. Chen, R. W. Murray, *Langmuir* **1999**, *15*, 682–689.
[25] M. J. Hostetler, S. J. Green, J. J. Stokes, R. W. Murray, *J. Am. Chem. Soc.* **1996**, *118*, 4212–4213.
[26] R. S. Ingram, M. J. Hostetler, R. W. Murray, *J. Am. Chem. Soc.* **1997**, *119*, 9175–9178.
[27] A. C. Templeton, W. P. Wuelfing, R. W. Murray, *Acc. Chem. Res.* **2000**, *33*, 27–36.
[28] M. J. Hostetler, J. E. Wingate, C. J. Zhong, J. E. Harris, R. W. Vachet, M. R. Clark, J. D. Londono, S. J. Green, J. J. Stokes, G. D. Wignall, G. L. Glish, M. D. Porter, N. D. Evans, R. W. Murray, *Langmuir* **1998**, *14*, 17–30.
[29] A. C. Templeton, M. J. Hostetler, C. T. Kraft, R. W. Murray, *J. Am. Chem. Soc.* **1998**, *120*, 1906–1911.
[30] M. J. Hostetler, A. C. Templeton, R. W. Murray, *Langmuir* **1999**, *15*, 3782–3789.
[31] O. Tzhayik, P. Sawant, S. Efrima, E. Kovalev, J. T. Klug, *Langmuir* **2002**, *18*, 3364–3369.
[32] L. A. J. Porter, D. Ji, S. L. Westcott, M. Graupe, R. S. Czernuszewicz, N. J. Halas, T. R. Lee, *Langmuir* **1998**, *14*, 7378–7386.
[33] T. Yonezawa, K. Yasui, N. Kimizuka, *Langmuir* **2001**, *17*, 271–273.
[34] A. Manna, P. L. Chen, H. Akiyama, T. X. Wei, K. Tamada, W. Knoll, *Chem. Mater.* **2003**, *15*, 20–28.
[35] K. Torigoe, K. Esumi, *J. Phys. Chem. B* **1999**, *103*, 2862–2866.
[36] R. Resch, C. Baur, A. Bugacov, B. E. Koel, P. M. Echternach, A. Madhukar, N. Montoya, A. A. G. Requicha, P. Will, *J. Phys. Chem. B* **1999**, *103*, 3647–3650.
[37] N. Félidj, J. Aubard, G. Lévi, J. R. Krenn, A. Hohenau, G. Schider, A. Leitner, F. R. Aussenegg, *Appl. Phys. Lett.* **2003**, *82*, 3095–3097.
[38] Y. Tan, Y. Li, D. Zhu, *Langmuir* **2002**, *18*, 3392–3395.
[39] R. Balasubramanian, B. Kim, S. L. Tripp, X. Wang, M. Lieberman, A. Wei, *Langmuir* **2002**, *18*, 3676–3681.
[40] X. M. Li, M. R. de Jong, K. Inoue, S. Shinkai, J. Huskens, D. N. Reinhoudt, *J. Mater. Chem.* **2001**, *11*, 1919–1923.
[41] W. W. Weare, S. M. Reed, M. G. Warner, J. E. Hutchison, *J. Am. Chem. Soc.* **2000**, *122*, 12890–12891.
[42] M. Yamamoto, M. Nakamoto, *Chem. Lett.* **2003**, *32*, 452–453.
[43] J. R. Heath, L. Brandt, D. V. Leff, *Langmuir* **1996**, *12*, 4723–4730.
[44] J. Heath, C. Knobler, D. Leff, *J. Phys. Chem. B* **1997**, *101*, 189–197.
[45] S. Gomez, K. Philippot, V. Collière, B. Chaudret, F. Senocq, P. Lecante, *Chem. Commun.* **2000**, 1945–1946.
[46] M. Bardaji, P. Uznanski, C. Amiens, B. Chaudret, A. Laguna, *Chem. Commun.* **2002**, 598–599.
[47] M. Green, P. A. O'Brien, *Chem. Commun.* **2000**, 183–184.
[48] P. R. Selvakannan, S. Mandal, S. Phadtare, R. Pasricha, M. Sastry, *Langmuir* **2003**, *19*, 3545–3549.
[49] A. Ahmad, S. Senapati, M. I. Khan, R. Kumar, M. Sastry, *Langmuir* **2003**, *19*, 3550–3553.
[50] N. Anton, T. F. Vandamme, *Pharm. Res.* **2011**, *28*, 978–985.

[51] F. Chen, G. Q. Xu, T. S. A. Hor, *Mater. Lett.* **2003**, *57*, 3282–3286.
[52] H. Otsuka, Y. Nagasaki, K. Kataoka, *Adv. Drug Deliv. Rev.* **2003**, *55*, 403–419.
[53] A. Manna, T. Imae, T. Yogo, K. Aoi, M. Okazaki, *J. Colloid Interface Sci.* **2002**, *256*, 297–303.
[54] F. Aliotta, V. Arcoleo, S. Buccoleri, G. La Manna, V. T. Liveri, *Thermochim. Acta* **1995**, *265*, 15–23.
[55] V. Arcoleo, V. T. Liveri, *Chem. Phys. Lett.* **1996**, *258*, 223–227.
[56] F. Porta, L. Prati, M. Rossi, G. Scarì, *Colloids Surf.* **2002**, *211*, 43–48.
[57] C. L. Chiang, *J. Colloid Surf. Sci.* **2001**, *239*, 334–341.
[58] C. L. Chiang, *J. Colloid Interface Sci.* **2000**, *230*, 60–66.
[59] N. R. Jana, L. Gearheart, C. J. Murphy, *Chem. Mater.* **2001**, *13*, 2313–2322.
[60] T. K. Sau, A. Pal, N. R. Jana, Z. L. Wang, T. Pal, *J. Nanopart. Res.* **2001**, *3*, 257–261.
[61] S. Meltzer, R. Resch, B. E. Koel, M. E. Thompson, A. Madhukar, A. A. G. Requicha, P. Will, *Langmuir* **2001**, *17*, 1713–1718.
[62] B. D. Busbee, S. O. Obare, C. J. Murphy, *Adv. Mater.* **2003**, *15*, 414–416.
[63] R. Guo, H. Wang, C. Peng, M. Shen, M. Pan, X. Cao, G. Zhang, X. Shi, *J. Phys. Chem. C* **2010**, *114*, 50–56.
[64] C. Peng, H. Wang, R. Guo, M. Shen, X. Cao, M. Zhu, G. Zhang, X. Shi, *J. Appl. Polym. Sci.* **2011**, *119*, 1673–1682.
[65] X. Shi, I. Lee, J. R. J. Baker, *J. Mater. Chem.* **2008**, *18*, 586–593.
[66] M. Shen, X. Shi, *Nanoscale* **2010**, *2*, 1027–1032.
[67] M. Shen, K. Sun, X. Shi, *Curr. Nanosci.* **2010**, *6*, 307–314.
[68] X. Shi, S. H. Wang, M. E. Van Antwerp, X. Chen, J. R. J. Baker, *Analyst* **2009**, *134*, 1373–1379.
[69] X. Shi, T. R. Ganser, K. Sun, L. P. Balogh, J. R. Baker Jr., *Nanotechnology* **2006**, *17*, 1072–1078.
[70] X. Shi, K. Sun, J. R. J. Baker, *J. Phys. Chem. C* **2008**, *112*, 8251–8258.
[71] C. Kojima, Y. Umeda, M. Ogawa, A. Harada, Y. Magata, K. Kono, *Nanotechnology* **2010**, *21*, 245104–245109.
[72] H. Wang, L. Zheng, C. Peng, R. Guo, M. Shen, X. Shi, G. Zhang, *Biomaterials* **2011**, *32*, 2979–2988.
[73] X. Shi, S. Wang, S. Meshinchi, M. Van Antwerp, X. Bi, I. Lee, B. J. R. Jr., *Small* **2007**, *3*, 1245–1252.
[74] R. Guo, H. Wang, C. Peng, M. Shen, L. Zheng, G. Zhang, X. Shi, *J. Mater. Chem.* **2011**, *21*, 5120–5127.
[75] X. Shi, S. Wang, H. Sun, J. R. J. Baker, *Soft Matter* **2007**, *3*, 71–74.
[76] S. Hong, A. U. Bielinska, A. Mecke, B. Keszler, J. L. Beals, X. Shi, L. Balogh, B. G. Orr, J. R. J. Baker, M. M. Banaszak Holl, *Bioconjug. Chem.* **2004**, *15*, 774–782.
[77] X. Shi, S. H. Wang, I. Lee, M. Shen, J. R. J. Baker, *Biopolymers* **2009**, *91*, 936–942.
[78] V. Kozlovskaya, E. Kharlampieva, B. P. Khanal, P. Manna, E. R. Zubarev, V. V. Tsukruk, *Chem. Mater.* **2008**, *20*, 7474–7485.
[79] L. Pei, K. Mori, M. Adachi, *Langmuir* **2004**, *20*, 7837–7843.
[80] H. Xia, S. Bai, J. Hartmann, D. Wang, *Langmuir* **2010**, *26*, 3585–3589.
[81] C. L. Nehl, H. Liao, J. H. Hafner, *Nano Lett.* **2006**, *6*, 683–688.
[82] X. Kou, Z. Sun, Z. Yang, H. Chen, J. Wang, *Langmuir* **2009**, *25*, 1692–1698.
[83] B. P. Khanal, E. R. Zubarev, *J. Am. Chem. Soc.* **2008**, *130*, 12634–12635.
[84] X. Xu, N. L. Rosi, Y. Wang, F. Huo, C. A. Mirkin, *J. Am. Chem. Soc.* **2006**, *128*, 9286–9287.
[85] C. C. Chen, C. H. Hsu, P. L. Kuo, *Langmuir* **2007**, *23*, 6801–6806.
[86] J. Chen, F. Saeki, B. J. Wiley, H. Cang, M. J. Cobb, Z. Y. Li, L. Au, H. Zhang, M. B. Kimmey, Li, Y. Xia, *Nano Lett.* **2005**, *5*, 473–477.
[87] http://physics.nist.gov/PhysRefData/XrayMassCoef, [Assessed 12 April **2011**].
[88] I. C. Sun, D. K. Eun, J. H. Na, S. Lee, I. J. Kim, I. C. Youn, C. Y. Ko, H. S. Kim, D. Lim, K. Choi, P. B. Messersmith, T. G. Park, S. Y. Kim, I. C. Kwon, K. Kim, C. H. Ahn, *Chem. Eur. J.* **2009**, *15*, 13341–13347.
[89] D. P. Cormode, E. Roessl, A. Thran, T. Skajaa, R. Gordon, J. P. Schlomka, V. Fuster, E. A. Fisher, W. J. Mulder, R. Proksa, Z. A. Fayad, *Radiology* **2010**, *256*, 774–782.
[90] E. Boote, G. Fent, V. Kattumuri, S. Casteel, K. Katti, N. Chanda, R. Kannan, K. Katti, R. Churchill, *Acad. Radiol.* **2010**, *17*, 410–417.
[91] N. Chanda, V. Kattumuri, R. Shukla, A. Zambre, K. Katti, A. Upendran, R. R. Kulkarni, P. Kan, G. M. Fent, S. W. Casteel, C. J. Smith, E. Boote, J. D. Robertson, C. Cutler, J. R. Lever, K. V. Katti, R. Kannan, *Proc. Natl. Acad. Sci. U. S. A.* **2010**, *107*, 8760–8765.
[92] O. C. Farokhzad, J. J. Cheng, B. A. Teply, I. Sherifi, S. Jon, P. W. Kantoff, J. P. Richie, R. Langer, *Proc. Natl. Acad. Sci. U. S. A.* **2006**, *103*, 6315–6320.
[93] H. F. Wang, T. B. Huff, D. A. Zweifel, W. He, P. S. Low, A. Wei, J. X. Cheng, *Proc. Natl. Acad. Sci. U. S. A.* **2005**, *102*, 15752–15756.
[94] C. C. Chen, Y. P. Lin, C. W. Wang, H. C. Tzeng, C. H. Wu, Y. C. Chen, C. P. Chen, L. C. Chen, Y. C. Wu, *J. Am. Chem. Soc.* **2006**, *128*, 3709–3715.
[95] A. G. Tkachenko, H. Xie, D. Coleman, W. Glomm, J. Ryan, M. F. Anderson, S. Franzen, D. L. Feldheim, *J. Am. Chem. Soc.* **2003**, *125*, 4700–4701.
[96] L. Loo, R. H. Guenther, V. R. Basnayake, S. A. Lommel, S. Franzen, *J. Am. Chem. Soc.* **2006**, *128*, 4502–4503.
[97] E. Oh, M. Y. Hong, D. Lee, S. H. Nam, H. C. Yoon, H. S. Kim, *J. Am. Chem. Soc.* **2005**, *127*, 3270–3271.
[98] K. Sokolov, J. Aaron, B. Hsu, D. Nida, A. Gillenwater, M. Follen, C. MacAulay, K Adler-Storthz, B. Korgel, M. Descour, R. Pasqualini, W. Arap, W. Lam, R Richards-Kortum, *Technol. Cancer Res. Treat.* **2003**, *2*, 491–504.
[99] K. K. Katti, V. Kattumuri, S. Bhaskaran, K. V. Katti, R. Kannan, *Int. J. Green Nanotechnol. Biomed.* **2009**, *1*, B53–B59.
[100] R. Kannan, V. Rahing, C. Cutler, R. Pandrapragada, K. K. Katti, V. Kattumuri, J. D. Robertson, S. J. Casteel, S. Jurisson, C. Smith, E. Boote, K. V. Katti, *J. Am. Chem. Soc.* **2006**, *128*, 11342–11343.
[101] S. Ahn, S.-Y. Jung, B. H. Kim, S. J. Lee, *Acta Biomater.* **2011**, *7*, 2139–2147.
[102] Z. Wang, L. Wu, W. Cai, *Chem. Eur. J.* **2010**, *16*, 1459–1463.
[103] B. Aydogan, J. Li, T. Rajh, A. Chaudhary, S. J. Chmura, C. Pelizzari, C. Wietholt, M. Kurtoglu, P. Redmond, *Mol. Imaging. Biol.* **2010**, *12*, 463–467.
[104] J. Li, A. Chaudhary, S. J. Chmura, C. Pelizzari, T. Rajh, C. Wietholt, M. Kurtoglu, B. Aydogan, *Phys. Med. Biol.* **2010**, *55*, 4389–4397.
[105] C. Xu, G. A. Tung, S. Sun, *Chem. Mater.* **2008**, *20*, 4167–4169.
[106] J. D. Trono, K. Mizuno, N. Yusa, T. Matsukawa, K. Yokoyama, M. Uesaka, *J. Radiat. Res.* **2011**, *52*, 103–109.
[107] R. H. Menk, E. Schültke, C. Hall, F. Arfelli, A. Astolfo, L. Rigon, A. Round, K. Ataelmannan, S. R. McDonald, B. H. J. Juurlink, *Nanomed.-Nanotechnol. Biol. Med.* **2011**, *7*, 647–654.
[108] D. Kim, M. K. Yu, T. S. Lee, J. J. Park, Y. Y. Jeong, S. Jon, *Nanotechnology* **2011**, *22*, 155101–155107.
[109] D. Cormode, Z. A. Fayad, *Imaging Med.* **2011**, *3*, 263–266.
[110] N. K. Devaraj, E. J. Keliher, G. M. Thurber, M. Nahrendorf, R. Weissleder, *Bioconjug. Chem.* **2009**, *20*, 397–401.
[111] X. Shao, H. Zhang, J. R. Rajian, D. L. Chamberland, P. S. Sherman, C. A. Quesada, A. E. Koch, N. A. Kotov, X. Wang, *ACS Nano* **2011**, *5*, 8967–8973.
[112] Y. Liu, M. Welch, *Bioconjug. Chem.* **2012**, *in press*.
[113] C. Alric, J. Taleb, G. L. Duc, C. Mandon, A. L. Billotey, C Meur-Herland, T. Brochard, F. Vocanson, M. Janier, P. Perriat, S. Roux, O. Tillement, *J. Am. Chem. Soc.* **2008**, *130*, 5908–15.

[114] H. K. Kim, H. Y. Jung, J. A. Park, M. I. Huh, J. C. Jung, Y. Chang, T. J. Kim, *J. Mater. Chem.* **2010**, *20*, 5411–5417.
[115] S. M. Nasiruzzaman, H. K. Kim, J. A. Park, Y. Chang, K. T. J., *Bull. Korean Chem. Soc.* **2010**, *31*, 1177–1181.
[116] J. A. Park, H. K. Kim, J. H. Kim, S. W. Jeong, J. C. Jung, G. H. Lee, J. Lee, Y. Chang, T. J. Kim, *Bioorg. Med. Chem. Lett.* **2010**, *20*, 2287–2291.
[117] Y. Song, X. Xu, K. W. MacRenaris, X. Q. Zhang, C. A. Mirkin, T. J. Meade, *Angew. Chem. Int. Edit.* **2009**, *48*, 9143–9147.
[118] D. Kim, J. W. Kim, Y. Y. Jeong, S. Jon, *Bull. Korean Chem. Soc.* **2009**, *30*, 1855–1857.
[119] M. M. van Schooneveld, D. P. Cormode, R. Koole, J. T. van Wijngaarden, C. Calcagno, T. Skajaa, J. Hilhorst, D. C. 't Hart, Z. A. Fayad, W. J. M. Mulder, A. Meijerink, *Contrast Media Mol Imaging* **2010**, *5*, 231–236.
[120] D. P. Cormode, T. Skajaa, M. M. van Schooneveld, R. Koole, P. Jarzyna, M. E. Lobatto, C. Calcagno, A. Barazza, R. E. Gordon, P. Zanzonico, E. A. Fisher, Z. A. Fayad, W. J. M. Mulder, *Nano Lett.* **2008**, *8*, 3715–3723.
[121] F. Voelcker, A. von Lichtenberg, *Munch. Med. Wschr.* **1906**, *53*, 105–106.
[122] A. A. Uhle, G. E. Pfahler, W. H. Mackinney, A. G. Miller, *Ann. Surg.* **1910**, *51*, 546–551.
[123] W. Braasch, *Urography*, Philadelphia and London: W. B. Saunders and Co, **1928**.
[124] S. E. Seltzer, D. F. Adams, M. A. Davis, S. J. Hessel, A. Havron, P. F. Judy, A. J. Paskins-Hurlburt, N. K. Hollenberg, *J. Comput. Assist. Tomogr.* **1981**, *5*, 370–374.
[125] M. Swick, *Surg. Clin. North Am.* **1978**, *58*, 977–994.
[126] S. E. Seltzer, D. F. Adams, M. A. Davis, S. J. Hessel, A. J. Paskins-Hurlburt, A. Havron, N. K. Hollenberg, *Invest. Radiol.* **1979**, *14*, 356.
[127] R. Eisenberg, *Radiology, An Illustrated History*, Morsby-Year Book: St. Louis, **1992**.
[128] K. Skrepetis, Febu, I. Siafakas, M. Lykourinas, *J. Endourology* **2001**, *15*, 691–696.
[129] P. V. Asharani, G. L. K. Mun, M. P. Hande, S. Valiyaveettil, *ACS Nano* **2009**, *3*, 279–90.
[130] S. Kittler, C. Greulich, J. Diendorf, M. Koller, M. Epple, *Chem. Mater.* **2010**, *22*, 4548–4554.
[131] C. M. Zhao, W. X. Wang, *Environ. Toxicol. Chem.* **2011**, *30*, 885–892.
[132] W. Lu, D. Senapati, S. Wang, O. Tovmachenko, A. K. Singh, H. Yu, P. C. Ray, *Chem. Phys. Lett.* **2010**, *487*, 92–96.
[133] H. Liu, H. Wang, R. Guo, X. Cao, J. Zhao, Y. Luo, M. Shen, G. Zhang, X. Shi, *Polym. Chem.* **2010**, *1*, 1677–1683.
[134] S.-W. Chou, Y.-H. Shau, P.-C. Wu, Y.-S. Yang, D.-B. Shieh, C.-C. Chen, *J. Am. Chem. Soc.* **2010**, *132*, 13270–13278.
[135] J. D. Abbatt, *Environ. Res.* **1979**, *18*, 6–12.
[136] R. H. Carrigan, *Ann. N. Y. Acad. Sci.* **1967**, *145*, 530–32.
[137] J. S. Ritter, I. N. Rattner, *Am. J. Roentgenol.* **1932**, *28*, 629–633.
[138] M. L. Janower, O. S. Miettinen, M. J. Flynn, *Radiology* **1972**, *103*, 13–20.
[139] J. D. Abbatt, *Annals of the New York Academy of Sciences* **1967**, *145*, 767–775.
[140] Y. Ito, M. Kojiro, T. Nakashima, T. Mori, *Cancer* **1988**, *62*, 1153–1162.
[141] R. J. W. van Kampen, F. L. G. Erdkamp, F. P. J. Peters, *Neth. J. Med.* **2007**, *65*, 279–282.
[142] D. Kessel, K. F. Robbins, M. L. Wilkinson, P. M. Smith, *Br. J. Radiol.* **1991**, *64*, 1067–1069.
[143] G. S. Lipshutz, T. V. Brennan, R. S. Warren, *J Am Coll Surg* **2002**, *195*, 713–18.
[144] W. B. Cannon, *Am. J. Physiol.* **1898**, *1*, 359–382.
[145] T. Rumpel, *Muenchen Med. Wschr.* **1897**, *44*, 421–421.
[146] O. Rabin, J. M. Perez, J. Grimm, G. Wojtkiewicz, R. Weissleder, *Nat. Mater.* **2006**, *5*, 118–122.
[147] B. P. Barnett, D. L. Kraitchman, C. Lauzon, C. A. Magee, P. Walczak, W. D. Gilson, A. Arepally, J. W. M. Bulte, *Mol. Pharm.* **2006**, *3*, 531–538.
[148] D. Pan, E. Roessl, J. P. Schlomka, S. D. Caruthers, A. Senpan, M. J. Scott, J. S. Allen, H. Zhang, G. Hu, P. J. Gaffney, E. T. Choi, V. Rasche, S. A. Wickline, R. Proksa, G. M. Lanza, *Angew. Chem. Int. Edit.* **2010**, *49*, 9635–9639.
[149] R. B. Dilley, J. A. Nadel, *Ann. Otol. Rhinol. Laryngol.* **1970**, *79*, 945–952.
[150] G. Gamsu, J. A. Nadel, *Cancer* **1972**, *30*, 1353–1357.
[151] G. Gamsu, A. Platzker, G. Gregory, P. Graf, J. A. Nadel, *Radiology* **1973**, *107*, 151–157.
[152] J. A. Nadel, W. G. Wolfe, P. D. Graf, J. E. Youker, N. Zamel, J. H. M. Austin, W. A. Hinchcliffe, R. H. Greenspan, R. R. Wright, *N. Engl. J. Med.* **1970**, *283*, 281–286.
[153] W. J. Dodds, H. I. Goldberg, S. Kohatsu, L. J. McCarthy, J. Nadel, F. F. Zboralske, *Invest. Radiol.* **1970**, *5*, 30–34.
[154] H. I. Goldberg, W. J. Dodds, E. H. Jenis, *Am. J. Roentgenol Radium Ther. Nucl. Med.* **1970**, *110*, 288–94.
[155] J. A. Nadel, W. J. Dodds, H. Goldberg, P. D. Graf, *Invest Radiol.* **1969**, *4*, 57–62.
[156] P. J. Bonitatibus, A. S. Torres, G. D. Goddard, P. F. FitzGerald, A. M. Kulkarni, *Chem. Commun.* **2010**, *46*, 8956–8958.
[157] M. H. Oh, N. Lee, H. Kim, S. P. Park, Y. Piao, J. Lee, S. W. Jun, W. K. Moon, S. H. Choi, T. Hyeon, *J. Am. Chem. Soc.* **2011**, *133*, 5508–15.
[158] D. C. Chan, H. W. Titus, K. H. Chung, H. Dixon, S. T. Wellinghoff, H. R. Rawls, *Dent. Mater.* **1999**, *15*, 219–222.
[159] B. Furman, H. R. Rawls, S. Wellinghoff, H. Dixon, J. Lankford, D. Nicolella, *Crit. Rev. Biomed. Eng.* **2000**, *28*, 439–443.
[160] H. Schulz, L. Mdler, S. E. Pratsinis, P. Burtscher, N. Moszner, *Adv. Func. Mater.* **2005**, *15*, 830–37.
[161] H. Schulz, B. Schimmoeller, S. E. Pratsinis, U. Salz, T. Bock, *J Dent.* **2008**, *36*, 579–87.
[162] S. T. Wellinghoff, H. Dixon, D. Nicolella, M. Fan, H. R. Rawls, *J. Dent. Res.* **1998**, *77*, 639 abstract 58.
[163] A. Havron, M. A. Davis, S. E. Seltzer, A. J Paskins-Hurlburt, S. J. Hessel, *J. Comput. Assist. Tomogr.* **1980**, *4*, 642–648.
[164] E. N. M. Cheung, R. D. A. Alvares, W. Oakden, R. Chaudhary, M. L. Hill, J. Pichaandi, G. C. H. Mo, C. Yip, P. M. MacDonald, G. J. Stanisz, F. C. J. M. van Veggel, R. S. Prosser, *Chem. Mater.* **2010**, *22*, 4728–4739.
[165] M. A. McDonald, K. L. Watkin, *Invest. Radiol.* **2003**, *38*, 305–310.
[166] K. L. Watkin, M. A. McDonald, *Acad. Radiol.* **2002**, *9*, S285–89.
[167] S. Santra, R. P. Bagwe, D. Dutta, J. T. Stanley, G. A. Walter, W. Tan, B. M. Moudgil, R. A. Mericle, *Adv. Mater.* **2005**, *17*, 2165–2169.
[168] W. Bult, P. R. Seevinck, G. C. Krijger, T. Visser, L. M. Kroon-Batenburg, C. J. Bakker, W. E. Hennink, A. D. van het Schip, J. F. W. Nijsen, *Pharm. Res.* **2009**, *26*, 1371–1378.
[169] W. Bult, R. Varkevisser, F. Soulimani, P. R. Seevinck, H. de Leeuw, C. J. Bakker, P. R. Luijten, A. D. van het Schip, W. E. Hennink, J. F. Nijsen, *Pharm. Res.* **2010**, *27*, 2205–2212.
[170] S. K. Nune, A. Tinsley, E. Boote, K. Katti, R. Kannan, in *NSTI Nanotech Santa Clara*, CA, USA May 20-24.
[171] J. M. Ashcroft, W. Gu, T. Zhang, S. M. Hughes, K. B. Hartman, C. Hofmann, A. G. Kanaras, D. A. Kilcoyne, M. Le Gros, Y. Yin, A. P. Alivisatos, *Chem. Commun.* **2008**, *21*, 2471–2473.
[172] M. Ajeesh, B. F. Francis, J. Annie, P. R. H. Varma, *J. Mater. Sci.-Mater. Med.* **2010**, *21*, 1427–1434.
[173] S. Santra, H. Yang, P. H. Holloway, J. T. Stanley, R. A. Mericle, *J. Am. Chem. Soc.* **2005**, *127*, 1656–1657.
[174] C. Schleh, M. Semmler-Behnke, J. Lipka, A. Wenk, S. Hirn, M. Sch Ffler, G. N. Schmid, U. Simon, W. G. Kreyling, *Nanotoxicology* **2012**, *6*, 36–48.